

8

Electron Levels in a Periodic Potential: General Properties

The Periodic Potential and Bloch's Theorem

Born-von Karman Boundary Condition

A Second Proof of Bloch's Theorem

Crystal Momentum, Band Index, and Velocity

The Fermi Surface

Density of Levels and van Hove Singularities

Because the ions in a perfect crystal are arranged in a regular periodic array, we are led to consider the problem of an electron in a potential $U(\mathbf{r})$ with the periodicity of the underlying Bravais lattice; i.e.,

$$U(\mathbf{r} + \mathbf{R}) = U(\mathbf{r}) \quad (8.1)$$

for all Bravais lattice vectors \mathbf{R} .

Since the scale of periodicity of the potential U ($\sim 10^{-8}$ cm) is the size of a typical de Broglie wavelength of an electron in the Sommerfeld free electron model, it is essential to use quantum mechanics in accounting for the effect of periodicity on electronic motion. In this chapter we shall discuss those properties of the electronic levels that depend only on the periodicity of the potential, without regard to its particular form. The discussion will be continued in Chapters 9 and 10 in two limiting cases of great physical interest that provide more concrete illustrations of the general results of this chapter. In Chapter 11 some of the more important methods for the detailed calculation of electronic levels are summarized. In Chapters 12 and 13 we shall discuss the bearing of these results on the problems of electronic transport theory first raised in Chapters 1 and 2, indicating how many of the anomalies of free electron theory (Chapter 3) are thereby removed. In Chapters 14 and 15 we shall examine the properties of specific metals that illustrate and confirm the general theory.

We emphasize at the outset that perfect periodicity is an idealization. Real solids are never absolutely pure, and in the neighborhood of the impurity atoms the solid is not the same as elsewhere in the crystal. Furthermore, there is always a slight temperature-dependent probability of finding missing or misplaced ions (Chapter 30) that destroy the perfect translational symmetry of even an absolutely pure crystal. Finally, the ions are not in fact stationary, but continually undergo thermal vibrations about their equilibrium positions.

These imperfections are all of great importance. They are, for example, ultimately responsible for the fact that the electrical conductivity of metals is not infinite. Progress is best made, however, by artificially dividing the problem into two parts: (a) the ideal fictitious perfect crystal, in which the potential is genuinely periodic, and (b) the effects on the properties of a hypothetical perfect crystal of all deviations from perfect periodicity, treated as small perturbations.

We also emphasize that the problem of electrons in a periodic potential does not arise only in the context of metals. Most of our general conclusions apply to all crystalline solids, and will play an important role in our subsequent discussions of insulators and semiconductors.

THE PERIODIC POTENTIAL

The problem of electrons in a solid is in principle a many-electron problem, for the full Hamiltonian of the solid contains not only the one-electron potentials describing the interactions of the electrons with the massive atomic nuclei, but also pair potentials describing the electron-electron interactions. In the independent electron approximation these interactions are represented by an effective one-electron potential $U(\mathbf{r})$. The problem of how best to choose this effective potential is a complicated one, which we shall return to in Chapters 11 and 17. Here we merely observe that whatever detailed form the one-electron effective potential may have, if the crystal is perfectly

periodic it must satisfy (8.1). From this fact alone many important conclusions can already be drawn.

Qualitatively, however, a typical crystalline potential might be expected to have the form shown in Figure 8.1, resembling the individual atomic potentials as the ion is approached closely and flattening off in the region between ions.

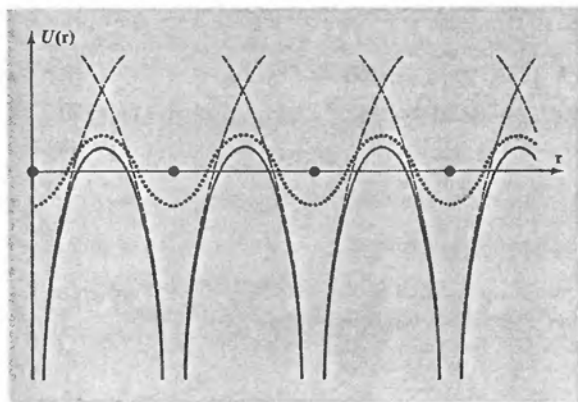


Figure 8.1

A typical crystalline periodic potential, plotted along a line of ions and along a line midway between a plane of ions. (Closed circles are the equilibrium ion sites; the solid curves give the potential along the line of ions; the dotted curves give the potential along a line between planes of ions; the dashed curves give the potential of single isolated ions.)

We are thus led to examine general properties of the Schrödinger equation for a single electron,

$$H\psi = \left(-\frac{\hbar^2}{2m} \nabla^2 + U(\mathbf{r}) \right) \psi = \varepsilon\psi, \quad (8.2)$$

that follow from the fact that the potential U has the periodicity (8.1). The free electron Schrödinger equation (2.4) is a special case of (8.2) (although, as we shall see, in some respects a very pathological one), zero potential being the simplest example of a periodic one.

Independent electrons, each of which obeys a one electron Schrödinger equation with a periodic potential, are known as *Bloch electrons* (in contrast to “free electrons,” to which Bloch electrons reduce when the periodic potential is identically zero). The stationary states of Bloch electrons have the following very important property as a general consequence of the periodicity of the potential U :

BLOCH'S THEOREM

Theorem.¹ The eigenstates ψ of the one-electron Hamiltonian $H = -\hbar^2\nabla^2/2m + U(\mathbf{r})$, where $U(\mathbf{r} + \mathbf{R}) = U(\mathbf{r})$ for all \mathbf{R} in a Bravais lattice, can be chosen to have the form of a plane wave times a function with the periodicity of the Bravais lattice:

$$\psi_{n\mathbf{k}}(\mathbf{r}) = e^{i\mathbf{k}\cdot\mathbf{r}} u_{n\mathbf{k}}(\mathbf{r}), \quad (8.3)$$

¹ The theorem was first proved by Floquet in the one-dimensional case, where it is frequently called *Floquet's theorem*.

where

$$u_{n\mathbf{k}}(\mathbf{r} + \mathbf{R}) = u_{n\mathbf{k}}(\mathbf{r}) \quad (8.4)$$

for all \mathbf{R} in the Bravais lattice.²

Note that Eqs. (8.3) and (8.4) imply that

$$\psi_{n\mathbf{k}}(\mathbf{r} + \mathbf{R}) = e^{i\mathbf{k} \cdot \mathbf{R}} \psi_{n\mathbf{k}}(\mathbf{r}). \quad (8.5)$$

Bloch's theorem is sometimes stated in this alternative form:³ the eigenstates of H can be chosen so that associated with each ψ is a wave vector \mathbf{k} such that

$$\psi(\mathbf{r} + \mathbf{R}) = e^{i\mathbf{k} \cdot \mathbf{R}} \psi(\mathbf{r}), \quad (8.6)$$

for every \mathbf{R} in the Bravais lattice.

We offer two proofs of Bloch's theorem, one from general quantum-mechanical considerations and one by explicit construction.⁴

FIRST PROOF OF BLOCH'S THEOREM

For each Bravais lattice vector \mathbf{R} we define a translation operator $T_{\mathbf{R}}$ which, when operating on any function $f(\mathbf{r})$, shifts the argument by \mathbf{R} :

$$T_{\mathbf{R}}f(\mathbf{r}) = f(\mathbf{r} + \mathbf{R}). \quad (8.7)$$

Since the Hamiltonian is periodic, we have

$$T_{\mathbf{R}}H\psi = H(\mathbf{r} + \mathbf{R})\psi(\mathbf{r} + \mathbf{R}) = H(\mathbf{r})\psi(\mathbf{r} + \mathbf{R}) = HT_{\mathbf{R}}\psi. \quad (8.8)$$

Because (8.8) holds identically for any function ψ , we have the operator identity

$$T_{\mathbf{R}}H = HT_{\mathbf{R}}. \quad (8.9)$$

In addition, the result of applying two successive translations does not depend on the order in which they are applied, since for any $\psi(\mathbf{r})$

$$T_{\mathbf{R}}T_{\mathbf{R}'}\psi(\mathbf{r}) = T_{\mathbf{R}'}T_{\mathbf{R}}\psi(\mathbf{r}) = \psi(\mathbf{r} + \mathbf{R} + \mathbf{R}'). \quad (8.10)$$

Therefore

$$T_{\mathbf{R}}T_{\mathbf{R}'} = T_{\mathbf{R}'}T_{\mathbf{R}} = T_{\mathbf{R} + \mathbf{R}'}. \quad (8.11)$$

Equations (8.9) and (8.11) assert that the $T_{\mathbf{R}}$ for all Bravais lattice vectors \mathbf{R} and the Hamiltonian H form a set of commuting operators. It follows from a fundamental theorem of quantum mechanics⁵ that the eigenstates of H can therefore be chosen to be simultaneous eigenstates of all the $T_{\mathbf{R}}$:

$$\begin{aligned} H\psi &= \varepsilon\psi, \\ T_{\mathbf{R}}\psi &= c(\mathbf{R})\psi. \end{aligned} \quad (8.12)$$

² The index n is known as the *band index* and occurs because for a given \mathbf{k} , as we shall see, there will be many independent eigenstates.

³ Equation (8.6) implies (8.3) and (8.4), since it requires the function $u(\mathbf{r}) = \exp(-i\mathbf{k} \cdot \mathbf{r})\psi(\mathbf{r})$ to have the periodicity of the Bravais lattice.

⁴ The first proof relies on some formal results of quantum mechanics. The second is more elementary, but also notationally more cumbersome.

⁵ See, for example, D. Park, *Introduction to the Quantum Theory*. McGraw-Hill, New York, 1964, p. 123.

The eigenvalues $c(\mathbf{R})$ of the translation operators are related because of the condition (8.11), for on the one hand

$$T_{\mathbf{R}} T_{\mathbf{R}'} \psi = c(\mathbf{R}) T_{\mathbf{R}} \psi = c(\mathbf{R}) c(\mathbf{R}') \psi, \quad (8.13)$$

while, according to (8.11),

$$T_{\mathbf{R}'} T_{\mathbf{R}} \psi = T_{\mathbf{R} + \mathbf{R}'} \psi = c(\mathbf{R} + \mathbf{R}') \psi. \quad (8.14)$$

It follows that the eigenvalues must satisfy

$$c(\mathbf{R} + \mathbf{R}') = c(\mathbf{R}) c(\mathbf{R}'). \quad (8.15)$$

Now let \mathbf{a}_i be three primitive vectors for the Bravais lattice. We can always write the $c(\mathbf{a}_i)$ in the form

$$c(\mathbf{a}_i) = e^{2\pi i x_i} \quad (8.16)$$

by a suitable choice⁶ of the x_i . It then follows by successive applications of (8.15) that if \mathbf{R} is a general Bravais lattice vector given by

$$\mathbf{R} = n_1 \mathbf{a}_1 + n_2 \mathbf{a}_2 + n_3 \mathbf{a}_3, \quad (8.17)$$

then

$$c(\mathbf{R}) = c(\mathbf{a}_1)^{n_1} c(\mathbf{a}_2)^{n_2} c(\mathbf{a}_3)^{n_3}. \quad (8.18)$$

But this is precisely equivalent to

$$c(\mathbf{R}) = e^{i\mathbf{k} \cdot \mathbf{R}}, \quad (8.19)$$

where

$$\mathbf{k} = x_1 \mathbf{b}_1 + x_2 \mathbf{b}_2 + x_3 \mathbf{b}_3 \quad (8.20)$$

and the \mathbf{b}_i are the reciprocal lattice vectors satisfying Eq. (5.4): $\mathbf{b}_i \cdot \mathbf{a}_j = 2\pi \delta_{ij}$.

Summarizing, we have shown that we can choose the eigenstates ψ of H so that for every Bravais lattice vector \mathbf{R} ,

$$T_{\mathbf{R}} \psi = \psi(\mathbf{r} + \mathbf{R}) = c(\mathbf{R}) \psi = e^{i\mathbf{k} \cdot \mathbf{R}} \psi(\mathbf{r}). \quad (8.21)$$

This is precisely Bloch's theorem, in the form (8.6).

THE BORN-VON KARMAN BOUNDARY CONDITION

By imposing an appropriate boundary condition on the wave functions we can demonstrate that the wave vector \mathbf{k} must be real, and arrive at a condition restricting the allowed values of \mathbf{k} . The condition generally chosen is the natural generalization of the condition (2.5) used in the Sommerfeld theory of free electrons in a cubical box. As in that case, we introduce the volume containing the electrons into the theory through a Born-von Karman boundary condition of macroscopic periodicity (page 33). Unless, however, the Bravais lattice is cubic and L is an integral multiple of the lattice constant a , it is not convenient to continue to work in a cubical volume of side L . Instead, it is more convenient to work in a volume commensurate with a

⁶ We shall see that for suitable boundary conditions the x_i must be real, but for now they can be regarded as general complex numbers.

primitive cell of the underlying Bravais lattice. We therefore generalize the periodic boundary condition (2.5) to

$$\psi(\mathbf{r} + N_i \mathbf{a}_i) = \psi(\mathbf{r}), \quad i = 1, 2, 3, \quad (8.22)$$

where the \mathbf{a}_i are three primitive vectors and the N_i are all integers of order $N^{1/3}$, where $N = N_1 N_2 N_3$ is the total number of primitive cells in the crystal.

As in Chapter 2, we adopt this boundary condition under the assumption that the bulk properties of the solid will not depend on the choice of boundary condition, which can therefore be dictated by analytical convenience.

Applying Bloch's theorem (8.6) to the boundary condition (8.22) we find that

$$\psi_{\mathbf{nk}}(\mathbf{r} + N_i \mathbf{a}_i) = e^{iN_i \mathbf{k} \cdot \mathbf{a}_i} \psi_{\mathbf{nk}}(\mathbf{r}), \quad i = 1, 2, 3, \quad (8.23)$$

which requires that

$$e^{iN_i \mathbf{k} \cdot \mathbf{a}_i} = 1, \quad i = 1, 2, 3. \quad (8.24)$$

When \mathbf{k} has the form (8.20), Eq. (8.24) requires that

$$e^{2\pi i N_i x_i} = 1, \quad (8.25)$$

and consequently we must have

$$x_i = \frac{m_i}{N_i}, \quad m_i \text{ integral}. \quad (8.26)$$

Therefore the general form for allowed Bloch wave vectors is⁷

$$\mathbf{k} = \sum_{i=1}^3 \frac{m_i}{N_i} \mathbf{b}_i, \quad m_i \text{ integral}. \quad (8.27)$$

It follows from (8.27) that the volume $\Delta \mathbf{k}$ of k -space per allowed value of \mathbf{k} is just the volume of the little parallelepiped with edges \mathbf{b}_i/N_i :

$$\Delta \mathbf{k} = \frac{\mathbf{b}_1}{N_1} \cdot \left(\frac{\mathbf{b}_2}{N_2} \times \frac{\mathbf{b}_3}{N_3} \right) = \frac{1}{N} \mathbf{b}_1 \cdot (\mathbf{b}_2 \times \mathbf{b}_3). \quad (8.28)$$

Since $\mathbf{b}_1 \cdot (\mathbf{b}_2 \times \mathbf{b}_3)$ is the volume of a reciprocal lattice primitive cell, Eq. (8.28) asserts that *the number of allowed wave vectors in a primitive cell of the reciprocal lattice is equal to the number of sites in the crystal.*

The volume of a reciprocal lattice primitive cell is $(2\pi)^3/v$, where $v = V/N$ is the volume of a direct lattice primitive cell, so Eq. (8.28) can be written in the alternative form:

$$\Delta \mathbf{k} = \frac{(2\pi)^3}{V}. \quad (8.29)$$

This is precisely the result (2.18) we found in the free electron case.

⁷ Note that (8.27) reduces to the form (2.16) used in free electron theory when the Bravais lattice is simple cubic, the \mathbf{a}_i are the cubic primitive vectors, and $N_1 = N_2 = N_3 = L/a$.

SECOND PROOF OF BLOCH'S THEOREM⁸

This second proof of Bloch's theorem illuminates its significance from a rather different point of view, which we shall exploit further in Chapter 9. We start with the observation that one can always expand any function obeying the Born-von Karman boundary condition (8.22) in the set of all plane waves that satisfy the boundary condition and therefore have wave vectors of the form (8.27).⁹

$$\psi(\mathbf{r}) = \sum_{\mathbf{q}} c_{\mathbf{q}} e^{i\mathbf{q} \cdot \mathbf{r}}. \quad (8.30)$$

Because the potential $U(\mathbf{r})$ is periodic in the lattice, its plane wave expansion will only contain plane waves with the periodicity of the lattice and therefore with wave vectors that are vectors of the reciprocal lattice.¹⁰

$$U(\mathbf{r}) = \sum_{\mathbf{k}} U_{\mathbf{k}} e^{i\mathbf{k} \cdot \mathbf{r}}. \quad (8.31)$$

The Fourier coefficients $U_{\mathbf{k}}$ are related to $U(\mathbf{r})$ by¹¹

$$U_{\mathbf{k}} = \frac{1}{v} \int_{\text{cell}} d\mathbf{r} e^{-i\mathbf{k} \cdot \mathbf{r}} U(\mathbf{r}). \quad (8.32)$$

Since we are at liberty to change the potential energy by an additive constant, we fix this constant by requiring that the spatial average U_0 of the potential over a primitive cell vanish:

$$U_0 = \frac{1}{v} \int_{\text{cell}} d\mathbf{r} U(\mathbf{r}) = 0. \quad (8.33)$$

Note that because the potential $U(\mathbf{r})$ is real, it follows from (8.32) that the Fourier coefficients satisfy

$$U_{-\mathbf{k}} = U_{\mathbf{k}}^*. \quad (8.34)$$

If we assume that the crystal has inversion symmetry¹² so that, for a suitable choice of origin, $U(\mathbf{r}) = U(-\mathbf{r})$, then (8.32) implies that $U_{\mathbf{k}}$ is real, and thus

$$U_{-\mathbf{k}} = U_{\mathbf{k}} = U_{\mathbf{k}}^* \quad (\text{for crystals with inversion symmetry}). \quad (8.35)$$

We now place the expansions (8.30) and (8.31) into the Schrödinger equation (8.2). The kinetic energy term gives

$$\frac{p^2}{2m} \psi = -\frac{\hbar^2}{2m} \nabla^2 \psi = \sum_{\mathbf{q}} \frac{\hbar^2}{2m} q^2 c_{\mathbf{q}} e^{i\mathbf{q} \cdot \mathbf{r}}. \quad (8.36)$$

⁸ Although more elementary than the first proof, the second is also notationally more complicated, and of importance primarily as a starting point for the approximate calculations of Chapter 9. The reader may therefore wish to skip it at this point.

⁹ We shall subsequently understand unspecified summations over \mathbf{k} to be over all wave vectors of the form (8.27) allowed by the Born-von Karman boundary condition.

¹⁰ A sum indexed by \mathbf{K} shall always be understood to run over all reciprocal lattice vectors.

¹¹ See Appendix D, where the relevance of the reciprocal lattice to Fourier expansions of periodic functions is discussed.

¹² The reader is invited to pursue the argument of this section (and Chapter 9) without the assumption of inversion symmetry, which is made solely to avoid inessential complications in the notation.

The term in the potential energy can be written¹³

$$\begin{aligned} U\psi &= \left(\sum_{\mathbf{K}} U_{\mathbf{K}} e^{i\mathbf{K}\cdot\mathbf{r}} \right) \left(\sum_{\mathbf{q}} c_{\mathbf{q}} e^{i\mathbf{q}\cdot\mathbf{r}} \right) \\ &= \sum_{\mathbf{K}\mathbf{q}} U_{\mathbf{K}} c_{\mathbf{q}} e^{i(\mathbf{K}+\mathbf{q})\cdot\mathbf{r}} = \sum_{\mathbf{K}\mathbf{q}'} U_{\mathbf{K}} c_{\mathbf{q}'-\mathbf{K}} e^{i\mathbf{q}'\cdot\mathbf{r}}. \end{aligned} \quad (8.37)$$

We change the names of the summation indices in (8.37)—from \mathbf{K} and \mathbf{q}' , to \mathbf{K}' and \mathbf{q} —so that the Schrödinger equation becomes

$$\sum_{\mathbf{q}} e^{i\mathbf{q}\cdot\mathbf{r}} \left\{ \left(\frac{\hbar^2}{2m} q^2 - \varepsilon \right) c_{\mathbf{q}} + \sum_{\mathbf{K}'} U_{\mathbf{K}'} c_{\mathbf{q}-\mathbf{K}'} \right\} = 0. \quad (8.38)$$

Since the plane waves satisfying the Born-von Karman boundary condition are an orthogonal set, the coefficient of each separate term in (8.38) must vanish,¹⁴ and therefore for all allowed wave vectors \mathbf{q} ,

$$\left(\frac{\hbar^2}{2m} q^2 - \varepsilon \right) c_{\mathbf{q}} + \sum_{\mathbf{K}'} U_{\mathbf{K}'} c_{\mathbf{q}-\mathbf{K}'} = 0. \quad (8.39)$$

It is convenient to write \mathbf{q} in the form $\mathbf{q} = \mathbf{k} - \mathbf{K}$, where \mathbf{K} is a reciprocal lattice vector chosen so that \mathbf{k} lies in the first Brillouin zone. Equation (8.39) becomes

$$\left(\frac{\hbar^2}{2m} (\mathbf{k} - \mathbf{K})^2 - \varepsilon \right) c_{\mathbf{k}-\mathbf{K}} + \sum_{\mathbf{K}'} U_{\mathbf{K}'} c_{\mathbf{k}-\mathbf{K}-\mathbf{K}'} = 0, \quad (8.40)$$

or, if we make the change of variables $\mathbf{K}' \rightarrow \mathbf{K}' - \mathbf{K}$,

$$\left(\frac{\hbar^2}{2m} (\mathbf{k} - \mathbf{K})^2 - \varepsilon \right) c_{\mathbf{k}-\mathbf{K}} + \sum_{\mathbf{K}'} U_{\mathbf{K}'-\mathbf{K}} c_{\mathbf{k}-\mathbf{K}'} = 0. \quad (8.41)$$

We emphasize that Eqs. (8.39) and (8.41) are nothing but restatements of the original Schrödinger equation (8.2) in momentum space, simplified by the fact that because of the periodicity of the potential, $U_{\mathbf{k}}$ is nonvanishing only when \mathbf{k} is a vector of the reciprocal lattice.

For fixed \mathbf{k} in the first Brillouin zone, the set of equations (8.41) for all reciprocal lattice vectors \mathbf{K} couples only those coefficients $c_{\mathbf{k}}$, $c_{\mathbf{k}-\mathbf{K}}$, $c_{\mathbf{k}-\mathbf{K}'}$, $c_{\mathbf{k}-\mathbf{K}''}$, . . . whose wave vectors differ from \mathbf{k} by a reciprocal lattice vector. Thus the original problem has separated into N independent problems: one for each allowed value of \mathbf{k} in the first Brillouin zone. Each such problem has solutions that are superpositions of plane waves containing only the wave vector \mathbf{k} and wave vectors differing from \mathbf{k} by a reciprocal lattice vector.

¹³ The last step follows from making the substitution $\mathbf{K} + \mathbf{q} = \mathbf{q}'$, and noting that because \mathbf{K} is a reciprocal lattice vector, summing over all \mathbf{q} of the form (8.27) is the same as summing over all \mathbf{q}' of that form.

¹⁴ This can also be deduced from Eq. (D.12), Appendix D, by multiplying (8.38) by the appropriate plane wave and integrating over the volume of the crystal.

Putting this information back into the expansion (8.30) of the wave function ψ , we see that if the wave vector \mathbf{q} only assumes the values \mathbf{k} , $\mathbf{k} - \mathbf{K}'$, $\mathbf{k} - \mathbf{K}''$, \dots , then the wave function will be of the form

$$\psi_{\mathbf{k}} = \sum_{\mathbf{K}} c_{\mathbf{k}-\mathbf{K}} e^{i(\mathbf{k}-\mathbf{K}) \cdot \mathbf{r}}. \quad (8.42)$$

If we write this as

$$\psi_{\mathbf{k}}(\mathbf{r}) = e^{i\mathbf{k} \cdot \mathbf{r}} \left(\sum_{\mathbf{K}} c_{\mathbf{k}-\mathbf{K}} e^{-i\mathbf{K} \cdot \mathbf{r}} \right), \quad (8.43)$$

then this is of the Bloch form (8.3) with the periodic function $u(\mathbf{r})$ given by¹⁵

$$u(\mathbf{r}) = \sum_{\mathbf{K}} c_{\mathbf{k}-\mathbf{K}} e^{-i\mathbf{K} \cdot \mathbf{r}}. \quad (8.44)$$

GENERAL REMARKS ABOUT BLOCH'S THEOREM

1. Bloch's theorem introduces a wave vector \mathbf{k} , which turns out to play the same fundamental role in the general problem of motion in a periodic potential that the free electron wave vector \mathbf{k} plays in the Sommerfeld theory. Note, however, that although the free electron wave vector is simply \mathbf{p}/\hbar , where \mathbf{p} is the momentum of the electron, in the Bloch case \mathbf{k} is not proportional to the electronic momentum. This is clear on general grounds, since the Hamiltonian does not have complete translational invariance in the presence of a nonconstant potential, and therefore its eigenstates will not be simultaneous eigenstates of the momentum operator. This conclusion is confirmed by the fact that the momentum operator, $\mathbf{p} = (\hbar/i) \nabla$, when acting on $\psi_{\mathbf{n}\mathbf{k}}$ gives

$$\begin{aligned} \frac{\hbar}{i} \nabla \psi_{\mathbf{n}\mathbf{k}} &= \frac{\hbar}{i} \nabla (e^{i\mathbf{k} \cdot \mathbf{r}} u_{\mathbf{n}\mathbf{k}}(\mathbf{r})) \\ &= \hbar \mathbf{k} \psi_{\mathbf{n}\mathbf{k}} + e^{i\mathbf{k} \cdot \mathbf{r}} \frac{\hbar}{i} \nabla u_{\mathbf{n}\mathbf{k}}(\mathbf{r}), \end{aligned} \quad (8.45)$$

which is not, in general, just a constant times $\psi_{\mathbf{n}\mathbf{k}}$; i.e., $\psi_{\mathbf{n}\mathbf{k}}$ is not a momentum eigenstate.

Nevertheless, in many ways $\hbar \mathbf{k}$ is a natural extension of \mathbf{p} to the case of a periodic potential. It is known as the *crystal momentum* of the electron, to emphasize this similarity, but one should not be misled by the name into thinking that $\hbar \mathbf{k}$ is a momentum, for it is not. An intuitive understanding of the dynamical significance of the wave vector \mathbf{k} can only be acquired when one considers the response of Bloch electrons to externally applied electromagnetic fields (Chapter 12). Only then does its full resemblance to \mathbf{p}/\hbar emerge. For the present, the reader should view \mathbf{k} as a quantum number characteristic of the translational symmetry of a periodic potential, just as the momentum \mathbf{p} is a quantum number characteristic of the fuller translational symmetry of free space.

2. The wave vector \mathbf{k} appearing in Bloch's theorem can always be confined to the first Brillouin zone (or to any other convenient primitive cell of the reciprocal

¹⁵ Note that there will be (infinitely) many solutions to the (infinite) set of equations (8.41) for a given \mathbf{k} . These are classified by the band index n (see footnote 2).

lattice). This is because any \mathbf{k}' not in the first Brillouin zone can be written as

$$\mathbf{k}' = \mathbf{k} + \mathbf{K} \quad (8.46)$$

where \mathbf{K} is a reciprocal lattice vector and \mathbf{k} does lie in the first zone. Since $e^{i\mathbf{k}' \cdot \mathbf{R}} = 1$ for any reciprocal lattice vector, if the Bloch form (8.6) holds for \mathbf{k}' , it will also hold for \mathbf{k} .

3. The index n appears in Bloch's theorem because for given \mathbf{k} there are many solutions to the Schrödinger equation. We noted this in the second proof of Bloch's theorem, but it can also be seen from the following argument:

Let us look for all solutions to the Schrödinger equation (8.2) that have the Bloch form

$$\psi(\mathbf{r}) = e^{i\mathbf{k} \cdot \mathbf{r}} u(\mathbf{r}), \quad (8.47)$$

where \mathbf{k} is fixed and u has the periodicity of the Bravais lattice. Substituting this into the Schrödinger equation, we find that u is determined by the eigenvalue problem

$$\begin{aligned} H_{\mathbf{k}} u_{\mathbf{k}}(\mathbf{r}) &= \left(\frac{\hbar^2}{2m} \left(\frac{1}{i} \nabla + \mathbf{k} \right)^2 + U(\mathbf{r}) \right) u_{\mathbf{k}}(\mathbf{r}) \\ &= \varepsilon_{\mathbf{k}} u_{\mathbf{k}}(\mathbf{r}) \end{aligned} \quad (8.48)$$

with boundary condition

$$u_{\mathbf{k}}(\mathbf{r}) = u_{\mathbf{k}}(\mathbf{r} + \mathbf{R}). \quad (8.49)$$

Because of the periodic boundary condition we can regard (8.48) as a Hermitian eigenvalue problem restricted to a single primitive cell of the crystal. Because the eigenvalue problem is set in a fixed finite volume, we expect on general grounds to find an infinite family of solutions with *discretely* spaced eigenvalues,¹⁶ which we label with the band index n .

Note that in terms of the eigenvalue problem specified by (8.48) and (8.49), the wave vector \mathbf{k} appears only as a parameter in the Hamiltonian $H_{\mathbf{k}}$. We therefore expect each of the energy levels, for given \mathbf{k} , to vary continuously as \mathbf{k} varies.¹⁷ In this way we arrive at a description of the levels of an electron in a periodic potential in terms of a family of continuous¹⁸ functions $\varepsilon_n(\mathbf{k})$.

4. Although the full set of levels can be described with \mathbf{k} restricted to a single primitive cell, it is often useful to allow \mathbf{k} to range through all of k -space, even though this gives a highly redundant description. Because the set of all wave functions and energy levels for two values of \mathbf{k} differing by a reciprocal lattice vector must be

¹⁶ Just as the problem of a free electron in a box of fixed finite dimensions has a set of discrete energy levels, the vibrational normal modes of a finite drumhead have a set of discrete frequencies, etc.

¹⁷ This expectation is implicit, for example, in ordinary perturbation theory, which is possible only because small changes in parameters in the Hamiltonian lead to small changes in the energy levels. In Appendix E the changes in the energy levels for small changes in \mathbf{k} are calculated explicitly.

¹⁸ The fact that the Born-von Karman boundary condition restricts \mathbf{k} to discrete values of the form (8.27) has no bearing on the continuity of $\varepsilon_n(\mathbf{k})$ as a function of a continuous variable \mathbf{k} , for the eigenvalue problem given by (8.48) and (8.49) makes no reference to the size of the whole crystal and is well defined for any \mathbf{k} . One should also note that the set of \mathbf{k} of the form (8.27) becomes dense in k -space in the limit of an infinite crystal.

identical, we can assign the indices n to the levels in such a way that for given n , the eigenstates and eigenvalues are periodic functions of \mathbf{k} in the reciprocal lattice:

$$\begin{aligned} \psi_{n, \mathbf{k} + \mathbf{K}}(\mathbf{r}) &= \psi_{n\mathbf{k}}(\mathbf{r}), \\ \varepsilon_{n, \mathbf{k} + \mathbf{K}} &= \varepsilon_{n\mathbf{k}}. \end{aligned} \quad (8.50)$$

This leads to a description of the energy levels of an electron in a periodic potential in terms of a family of continuous functions $\varepsilon_{n\mathbf{k}}$ (or $\varepsilon_n(\mathbf{k})$), each with the periodicity of the reciprocal lattice. The information contained in these functions is referred to as the *band structure* of the solid.

For each n , the set of electronic levels specified by $\varepsilon_n(\mathbf{k})$ is called an *energy band*. The origin of the term "band" will emerge in Chapter 10. Here we only note that because each $\varepsilon_n(\mathbf{k})$ is periodic in \mathbf{k} and continuous, it has an upper and lower bound, so that all the levels $\varepsilon_n(\mathbf{k})$ lie in the band of energies lying between these limits.

5. It can be shown quite generally (Appendix E) that an electron in a level specified by band index n and wave vector \mathbf{k} has a nonvanishing mean velocity, given by

$$\mathbf{v}_n(\mathbf{k}) = \frac{1}{\hbar} \nabla_{\mathbf{k}} \varepsilon_n(\mathbf{k}). \quad (8.51)$$

This is a most remarkable fact. It asserts that there are stationary (i.e., time-independent) levels for an electron in a periodic potential in which, in spite of the interaction of the electron with the fixed lattice of ions, it moves forever without any degradation of its mean velocity. This is in striking contrast to the idea of Drude that collisions were simply encounters between the electron and a static ion. Its implications are of fundamental importance, and will be explored in Chapters 12 and 13.

THE FERMI SURFACE

The ground state of N free electrons¹⁹ is constructed by occupying all one-electron levels \mathbf{k} with energies $\varepsilon(\mathbf{k}) = \hbar^2 k^2 / 2m$ less than ε_F , where ε_F is determined by requiring the total number of one-electron levels with energies less than ε_F to be equal to the total number of electrons (Chapter 2).

The ground state of N Bloch electrons is similarly constructed, except that the one-electron levels are now labeled by the quantum numbers n and \mathbf{k} , $\varepsilon_n(\mathbf{k})$ does not have the simple explicit free electron form, and \mathbf{k} must be confined to a single primitive cell of the reciprocal lattice if each level is to be counted only once. When the lowest of these levels are filled by a specified number of electrons, two quite distinct types of configuration can result:

¹⁹ We shall not distinguish notationally between the number of conduction electrons and the number of primitive cells when it is clear from the context which is meant; they are equal, however, only in a monovalent monatomic Bravais lattice (e.g., the alkali metals).

1. A certain number of bands may be completely filled, all others remaining empty. The difference in energy between the highest occupied level and the lowest unoccupied level (i.e., between the "top" of the highest occupied band and the "bottom" of the lowest empty band) is known as the *band gap*. We shall find that solids with a band gap greatly in excess of $k_B T$ (T near room temperature) are insulators (Chapter 12). If the band gap is comparable to $k_B T$, the solid is known as an *intrinsic semiconductor* (Chapter 28). Because the number of levels in a band is equal to the number of primitive cells in the crystal (page 136) and because each level can accommodate two electrons (one of each spin), a configuration with a band gap can arise (though it need not) only if the number of electrons per primitive cell is even.
2. A number of bands may be partially filled. When this occurs, the energy of the highest occupied level, the Fermi energy ϵ_F , lies within the energy range of one or more bands. For each partially filled band there will be a surface in k -space separating the occupied from the unoccupied levels. The set of all such surfaces is known as the *Fermi surface*, and is the generalization to Bloch electrons of the free electron Fermi sphere. The parts of the Fermi surface arising from individual partially filled bands are known as *branches* of the Fermi surface.²⁰ We shall see (Chapter 12) that a solid has metallic properties provided that a Fermi surface exists.

Analytically, the branch of the Fermi surface in the n th band is that surface in k -space (if there is one) determined by²¹

$$\epsilon_n(\mathbf{k}) = \epsilon_F. \quad (8.52)$$

Thus the Fermi surface is a constant energy surface (or set of constant energy surfaces) in k -space, just as the more familiar equipotentials of electrostatic theory are constant energy surfaces in real space.

Since the $\epsilon_n(\mathbf{k})$ are periodic in the reciprocal lattice, the complete solution to (8.52) for each n is a k -space surface with the periodicity of the reciprocal lattice. When a branch of the Fermi surface is represented by the full periodic structure, it is said to be described in a *repeated zone scheme*. Often, however, it is preferable to take just enough of each branch of the Fermi surface so that every physically distinct level is represented by just one point of the surface. This is achieved by representing each branch by that portion of the full periodic surface contained within a single primitive cell of the reciprocal lattice. Such a representation is described as a *reduced zone*

²⁰ In many important cases the Fermi surface is entirely within a single band, and generally it is found to lie within a fairly small number of bands (Chapter 15).

²¹ If ϵ_F is generally defined as the energy separating the highest occupied from the lowest unoccupied level, then it is not uniquely specified in a solid with an energy gap, since any energy in the gap meets this test. People nevertheless speak of "the Fermi energy" of an intrinsic semiconductor. What they mean is the chemical potential, which is well defined at any nonzero temperature (Appendix B). As $T \rightarrow 0$, the chemical potential of a solid with an energy gap approaches the energy at the middle of the gap (page 575), and one sometimes finds it asserted that this is the "Fermi energy" of a solid with a gap. With either the correct (undetermined) or colloquial definition of ϵ_F , Eq. (8.52) asserts that solids with a gap have no Fermi surface.

scheme. The primitive cell chosen is often, but not always, the first Brillouin zone.

Fermi surface geometry and its physical implications will be illustrated in many of the following chapters, particularly Chapters 9 and 15.

DENSITY OF LEVELS²²

One must often calculate quantities that are weighted sums over the electronic levels of various one-electron properties. Such quantities are of the form²³

$$Q = 2 \sum_{n,\mathbf{k}} Q_n(\mathbf{k}), \quad (8.53)$$

where for each n the sum is over all allowed \mathbf{k} giving physically distinct levels, i.e., all \mathbf{k} of the form (8.27) lying in a single primitive cell.²⁴

In the limit of a large crystal the allowed values (8.27) of \mathbf{k} get very close together, and the sum may be replaced with an integral. Since the volume of k -space per allowed \mathbf{k} (Eq. (8.29)) has the same value as in the free electron case, the prescription derived in the free electron case (Eq. (2.29)) remains valid, and we find that²⁵

$$q = \lim_{V \rightarrow \infty} \frac{Q}{V} = 2 \sum_n \int \frac{d\mathbf{k}}{(2\pi)^3} Q_n(\mathbf{k}), \quad (8.54)$$

where the integral is over a primitive cell.

If, as is often the case,²⁶ $Q_n(\mathbf{k})$ depends on n and \mathbf{k} only through the energy $\varepsilon_n(\mathbf{k})$, then in further analogy to the free electron case one can define a density of levels per unit volume (or "density of levels" for short) $g(\varepsilon)$ so that q has the form (cf. (2.60)):

$$q = \int d\varepsilon g(\varepsilon) Q(\varepsilon). \quad (8.55)$$

Comparing (8.54) and (8.55) we find that

$$g(\varepsilon) = \sum_n g_n(\varepsilon), \quad (8.56)$$

where $g_n(\varepsilon)$, the density of levels in the n th band, is given by

$$g_n(\varepsilon) = \int \frac{d\mathbf{k}}{4\pi^3} \delta(\varepsilon - \varepsilon_n(\mathbf{k})), \quad (8.57)$$

where the integral is over any primitive cell.

²² The reader can, without loss of continuity, skip this section at a first reading, referring back to it in subsequent chapters when necessary.

²³ The factor 2 is because each level specified by n and \mathbf{k} can accommodate two electrons of opposite spin. We assume that $Q_n(\mathbf{k})$ does not depend on the electron spin s . If it does, the factor 2 must be replaced by a sum on s .

²⁴ The functions $Q_n(\mathbf{k})$ usually have the periodicity of the reciprocal lattice, so the choice of primitive cell is immaterial.

²⁵ See page 37 for the appropriate cautionary remarks.

²⁶ For example, if q is the electronic number density n , then $Q(\varepsilon) = f(\varepsilon)$, where f is the Fermi function; if q is the electronic energy density u , then $Q(\varepsilon) = \varepsilon f(\varepsilon)$.

An alternative representation of the density of levels can be constructed by noting that, as in the free electron case (Eq. (2.62)):

$$g_n(\varepsilon) d\varepsilon = (2/V) \times \begin{array}{l} \text{(the number of allowed wave vectors} \\ \text{in the } n\text{th band in the energy range} \\ \text{from } \varepsilon \text{ to } \varepsilon + d\varepsilon). \end{array} \quad (8.58)$$

The number of allowed wave vectors in the n th band in this energy range is just the volume of a k -space primitive cell, with $\varepsilon \leq \varepsilon_n(\mathbf{k}) \leq \varepsilon + d\varepsilon$, divided by the volume per allowed wave vector, $\Delta\mathbf{k} = (2\pi)^3/V$. Thus

$$g_n(\varepsilon) d\varepsilon = \int \frac{d\mathbf{k}}{4\pi^3} \times \begin{cases} 1, & \varepsilon \leq \varepsilon_n(\mathbf{k}) \leq \varepsilon + d\varepsilon, \\ 0, & \text{otherwise} \end{cases} \quad (8.59)$$

Since $d\varepsilon$ is infinitesimal, this can also be expressed as a surface integral. Let $S_n(\varepsilon)$ be the portion of the surface $\varepsilon_n(\mathbf{k}) = \varepsilon$ lying within the primitive cell, and let $\delta k(\mathbf{k})$ be the perpendicular distance between the surfaces $S_n(\varepsilon)$ and $S_n(\varepsilon + d\varepsilon)$ at the point \mathbf{k} . Then (Figure 8.2):

$$g_n(\varepsilon) d\varepsilon = \int_{S_n(\varepsilon)} \frac{dS}{4\pi^3} \delta k(\mathbf{k}). \quad (8.60)$$

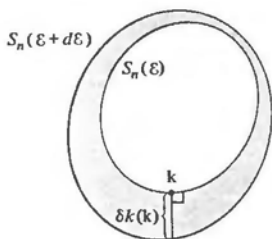


Figure 8.2

An illustration in two dimensions of the construction expressed in Eq. (8.60). The closed curves are the two constant-energy surfaces, the required area is that lying between them (shaded), and the distance $\delta k(\mathbf{k})$ is indicated for a particular \mathbf{k} .

To find an explicit expression for $\delta k(\mathbf{k})$ note that, since $S_n(\varepsilon)$ is a surface of constant energy, the k -gradient of $\varepsilon_n(\mathbf{k})$, $\nabla\varepsilon_n(\mathbf{k})$, is a vector normal to that surface whose magnitude is equal to the rate of change of $\varepsilon_n(\mathbf{k})$ in the normal direction; i.e.,

$$\varepsilon + d\varepsilon = \varepsilon + |\nabla\varepsilon_n(\mathbf{k})| \delta k(\mathbf{k}), \quad (8.61)$$

and hence

$$\delta k(\mathbf{k}) = \frac{d\varepsilon}{|\nabla\varepsilon_n(\mathbf{k})|}. \quad (8.62)$$

Substituting (8.62) into (8.60), we arrive at the form

$$g_n(\varepsilon) = \int_{S_n(\varepsilon)} \frac{dS}{4\pi^3} \frac{1}{|\nabla\varepsilon_n(\mathbf{k})|} \quad (8.63)$$

which gives an explicit relation between the density of levels and the band structure.

Equation (8.63) and the analysis leading to it will be applied in subsequent chapters.²⁷ Here we only note the following quite general property of the density of levels:

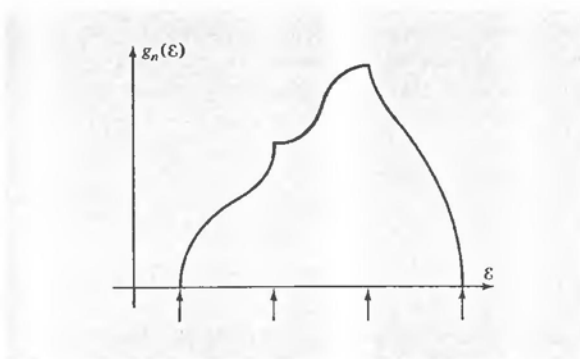
Because $\varepsilon_n(\mathbf{k})$ is periodic in the reciprocal lattice, bounded above and below for each n , and, in general, everywhere differentiable, there must be values of \mathbf{k} in each primitive cell at which $|\nabla\varepsilon| = 0$. For example, the gradient of a differentiable function vanishes at local maxima and minima, but the boundedness and periodicity of each $\varepsilon_n(\mathbf{k})$ insure that for each n there will be at least one maximum and minimum in each primitive cell.²⁸

When the gradient of ε_n vanishes, the integrand in the density of levels (8.63) diverges. It can be shown that in three dimensions²⁹ such singularities are integrable, yielding finite values for g_n . However, they do result in divergences of the slope, $dg_n/d\varepsilon$. These are known as *van Hove singularities*.³⁰ They occur at values of ε for which the constant energy surface $S_n(\varepsilon)$ contains points at which $\nabla\varepsilon_n(\mathbf{k})$ vanishes. Since derivatives of the density of levels at the Fermi energy enter into all terms but the first in the Sommerfeld expansion,³¹ one must be on guard for anomalies in low-temperature behavior if there are points of vanishing $\nabla\varepsilon_n(\mathbf{k})$ on the Fermi surface.

Typical van Hove singularities are shown in Figure 8.3 and are examined in Problem 2, Chapter 9.

Figure 8.3

Characteristic van Hove singularities in the density of levels, indicated by arrows at right angles to the ε -axis.



This concludes our discussion of the general features of one-electron levels in a periodic potential.³² In the following two chapters we consider two very important, but quite different, limiting cases, which provide concrete illustrations of the rather abstract discussions in this chapter.

²⁷ See also Problem 2.

²⁸ A very general analysis of how many points of vanishing gradient must occur is fairly complex. See, for example, G. Weinreich, *Solids*, Wiley, New York, 1965, pp. 73–79.

²⁹ In one dimension $g_n(\varepsilon)$ itself will be infinite at a van Hove singularity.

³⁰ Essentially the same singularities occur in the theory of lattice vibrations. See Chapter 23.

³¹ See, for example, Problem 2f, Chapter 2.

³² Problem 1 pursues the general analysis somewhat further in the tractable but somewhat misleading case of a one-dimensional periodic potential.

PROBLEMS

1. *Periodic Potentials in One Dimension*

The general analysis of electronic levels in a periodic potential, independent of the detailed features of that potential, can be carried considerably further in one dimension. Although the one-dimensional case is in many respects atypical (there is no need for a concept of a Fermi surface) or misleading (the possibility—indeed, in two and three dimensions the likelihood—of band overlap disappears), it is nevertheless reassuring to see some of the features of three-dimensional band structure we shall describe through approximate calculations, in Chapters 9, 10, and 11, emerging from an exact treatment in one dimension.

Consider, then, a one-dimensional periodic potential $U(x)$ (Figure 8.4). It is convenient to view the ions as residing at the minima of U , which we take to define the zero of energy. We choose to view the periodic potential as a superposition of potential barriers $v(x)$ of width a , centered at the points $x = \pm na$ (Figure 8.5):

$$U(x) = \sum_{n=-\infty}^{\infty} v(x - na). \quad (8.64)$$

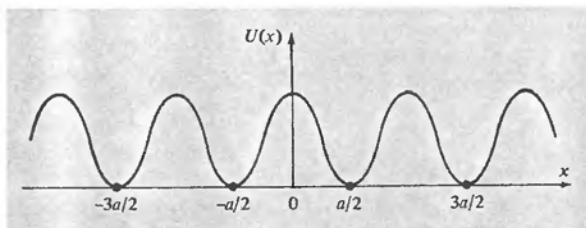


Figure 8.4

A one-dimensional periodic potential $U(x)$. Note that the ions occupy the positions of a Bravais lattice of lattice constant a . It is convenient to take these points as having coordinates $(n + \frac{1}{2})a$, and to choose the zero of potential to occur at the position of the ion.

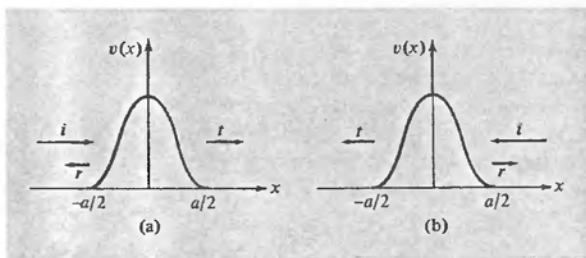


Figure 8.5

Illustrating particles incident from the left (a) and right (b) on a single one of the barriers separating neighboring ions in the periodic potential of Figure 8.4. The incident, transmitted, and reflected waves are indicated by arrows along the direction of propagation, proportional to the corresponding amplitudes.

The term $v(x - na)$ represents the potential barrier against an electron tunneling between the ions on opposite sides of the point na . For simplicity we assume that $v(x) = v(-x)$ (the one-dimensional analogue of the inversion symmetry we assumed above), but we make no other assumptions about v , so the form of the periodic potential U is quite general.

The band structure of the one-dimensional solid can be expressed quite simply in terms of the properties of an electron in the presence of a single-barrier potential $v(x)$. Consider therefore an electron incident from the left on the potential barrier $v(x)$ with energy³³ $\varepsilon = \hbar^2 K^2/2m$. Since $v(x) = 0$ when $|x| \geq a/2$, in these regions the wave function $\psi_l(x)$ will have the form

$$\begin{aligned}\psi_l(x) &= e^{iKx} + r e^{-iKx}, & x \leq -\frac{a}{2}, \\ &= t e^{iKx}, & x \geq \frac{a}{2}.\end{aligned}\quad (8.65)$$

This is illustrated schematically in Figure 8.5a.

The transmission and reflection coefficients t and r give the probability amplitude that the electron will tunnel through or be reflected from the barrier; they depend on the incident wave vector K in a manner determined by the detailed features of the barrier potential v . However, one can deduce many properties of the band structure of the periodic potential U by appealing only to very general properties of t and r . Because v is even, $\psi_r(x) = \psi_l(-x)$ is also a solution to the Schrödinger equation with energy ε . From (8.65) it follows that $\psi_r(x)$ has the form

$$\begin{aligned}\psi_r(x) &= t e^{-iKx}, & x \leq -\frac{a}{2}, \\ &= e^{-iKx} + r e^{iKx}, & x \geq \frac{a}{2}.\end{aligned}\quad (8.66)$$

Evidently this describes a particle incident on the barrier from the right, as depicted in Figure 8.5b.

Since ψ_l and ψ_r are two independent solutions to the single-barrier Schrödinger equation with the same energy, any other solution with that energy will be a linear combination³⁴ of these two: $\psi = A\psi_l + B\psi_r$. In particular, since the crystal Hamiltonian is identical to that for a single ion in the region $-a/2 \leq x \leq a/2$, any solution to the crystal Schrödinger equation with energy ε must be a linear combination of ψ_l and ψ_r in that region:

$$\psi(x) = A\psi_l(x) + B\psi_r(x), \quad -\frac{a}{2} \leq x \leq \frac{a}{2}. \quad (8.67)$$

Now Bloch's theorem asserts that ψ can be chosen to satisfy

$$\psi(x + a) = e^{ika}\psi(x), \quad (8.68)$$

for suitable k . Differentiating (8.68) we also find that $\psi' = d\psi/dx$ satisfies

$$\psi'(x + a) = e^{ika}\psi'(x). \quad (8.69)$$

(a) By imposing the conditions (8.68) and (8.69) at $x = -a/2$, and using (8.65) to (8.67), show that the energy of the Bloch electron is related to its wave vector k by:

$$\cos ka = \frac{t^2 - r^2}{2t} e^{ika} + \frac{1}{2t} e^{-ika}, \quad \varepsilon = \frac{\hbar^2 K^2}{2m}. \quad (8.70)$$

Verify that this gives the right answer in the free electron case ($v \equiv 0$).

³³ Note: in this problem K is a continuous variable and has nothing to do with the reciprocal lattice.

³⁴ A special case of the general theorem that there are n independent solutions to an n th-order linear differential equation.

Equation (8.70) is more informative when one supplies a little more information about the transmission and reflection coefficients. We write the complex number t in terms of its magnitude and phase:

$$t = |t| e^{i\delta}. \quad (8.71)$$

The real number δ is known as the phase shift, since it specifies the change in phase of the transmitted wave relative to the incident one. Electron conservation requires that the probability of transmission plus the probability of reflection be unity:

$$1 = |t|^2 + |r|^2. \quad (8.72)$$

This, and some other useful information, can be proved as follows. Let ϕ_1 and ϕ_2 be any two solutions to the one-barrier Schrödinger equation with the same energy:

$$-\frac{\hbar^2}{2m} \phi_i'' + v\phi_i = \frac{\hbar^2 K^2}{2m} \phi_i, \quad i = 1, 2. \quad (8.73)$$

Define $w(\phi_1, \phi_2)$ (the "Wronskian") by

$$w(\phi_1, \phi_2) = \phi_1'(x)\phi_2(x) - \phi_1(x)\phi_2'(x). \quad (8.74)$$

(b) Prove that w is independent of x by deducing from (8.73) that its derivative vanishes.

(c) Prove (8.72) by evaluating $w(\psi_l, \psi_l^*)$ for $x \leq -a/2$ and $x \geq a/2$, noting that because $v(x)$ is real ψ_l^* will be a solution to the same Schrödinger equation as ψ_l .

(d) By evaluating $w(\psi_l, \psi_l^*)$ prove that rt^* is pure imaginary, so r must have the form

$$r = \pm i |r| e^{i\delta}, \quad (8.75)$$

where δ is the same as in (8.71).

(e) Show as a consequence of (8.70), (8.72), and (8.75) that the energy and wave vector of the Bloch electron are related by

$$\frac{\cos(Ka + \delta)}{|t|} = \cos ka, \quad \varepsilon = \frac{\hbar^2 K^2}{2m}. \quad (8.76)$$

Since $|t|$ is always less than one, but approaches unity for large K (the barrier becomes increasingly less effective as the incident energy grows), the left side of (8.76) plotted against K has the structure depicted in Figure 8.6. For a given k , the allowed values of K (and hence the allowed energies $\varepsilon(k) = \hbar^2 K^2/2m$) are given by the intersection of the curve in Figure 8.6 with the horizontal line of height $\cos(ka)$. Note that values of K in the neighborhood of those satisfying

$$Ka + \delta = n\pi \quad (8.77)$$

give $|\cos(Ka + \delta)|/|t| > 1$, and are therefore not allowed for any k . The corresponding regions of energy are the energy gaps. If δ is a bounded function of K (as is generally the case), then there will be infinitely many regions of forbidden energy, and also infinitely many regions of allowed energies for each value of k .

(f) Suppose the barrier is very weak (so that $|t| \approx 1$, $|r| \approx 0$, $\delta \approx 0$). Show that the energy gaps are then very narrow, the width of the gap containing $K = n\pi/a$ being

$$\varepsilon_{\text{gap}} \approx 2\pi n \frac{\hbar^2}{ma^2} |r|. \quad (8.78)$$

(g) Suppose the barrier is very strong, so that $|t| \approx 0$, $|r| \approx 1$. Show that the allowed bands

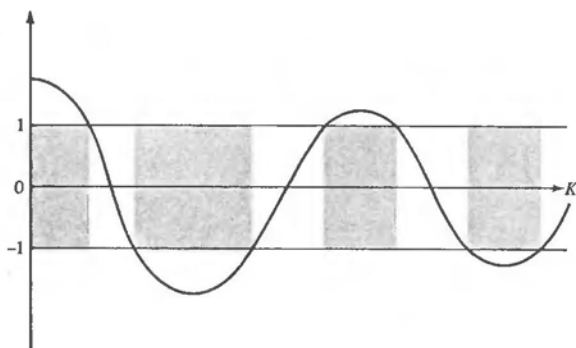


Figure 8.6

Characteristic form of the function $\cos(Ka + \delta)/|t|$. Because $|t(K)|$ is always less than unity the function will exceed unity in magnitude in the neighborhood of solutions to $Ka + \delta(K) = n\pi$. Equation (8.76) can be satisfied for real k if and only if the function is less than unity in magnitude. Consequently there will be allowed (unshaded) and forbidden (shaded) regions of K (and therefore of $\epsilon = \hbar^2 K^2/2m$). Note that when $|t|$ is very near unity (weak potential) the forbidden regions will be narrow, but if $|t|$ is very small (strong potential) the allowed regions will be narrow.

of energies are then very narrow, with widths

$$\epsilon_{\max} - \epsilon_{\min} = O(|t|). \quad (8.79)$$

(h) As a concrete example, one often considers the case in which $v(x) = g\delta(x)$, where $\delta(x)$ is the Dirac delta function (a special case of the "Kronig-Penney model"). Show that in this case

$$\cot \delta = -\frac{\hbar^2 K}{mg}, \quad |t| = \cos \delta. \quad (8.80)$$

This model is a common textbook example of a one-dimensional periodic potential. Note, however, that most of the structure we have established is, to a considerable degree, independent of the particular functional dependence of $|t|$ and δ on K .

2. Density of Levels

(a) In the free electron case the density of levels at the Fermi energy can be written in the form (Eq. (2.64)) $g(\epsilon_F) = mk_F/\hbar^2\pi^2$. Show that the general form (8.63) reduces to this when $\epsilon_n(\mathbf{k}) = \hbar^2 k^2/2m$ and the (spherical) Fermi surface lies entirely within a primitive cell.

(b) Consider a band in which, for sufficiently small k , $\epsilon_n(\mathbf{k}) = \epsilon_0 + (\hbar^2/2)(k_x^2/m_x + k_y^2/m_y + k_z^2/m_z)$ (as might be the case in a crystal of orthorhombic symmetry) where m_x , m_y , and m_z are positive constants. Show that if ϵ is close enough to ϵ_0 that this form is valid, then $g_n(\epsilon)$ is proportional to $(\epsilon - \epsilon_0)^{1/2}$, so its derivative becomes infinite (van Hove singularity) as ϵ approaches the band minimum. (*Hint*: Use the form (8.57) for the density of levels.) Deduce from this that if the quadratic form for $\epsilon_n(\mathbf{k})$ remains valid up to ϵ_F , then $g_n(\epsilon_F)$ can be written in the obvious generalization of the free electron form (2.65):

$$g_n(\epsilon_F) = \frac{3}{2} \frac{n}{\epsilon_F - \epsilon_0} \quad (8.81)$$

where n is the contribution of the electrons in the band to the total electronic density.

(c) Consider the density of levels in the neighborhood of a saddle point, where $\varepsilon_n(\mathbf{k}) = \varepsilon_0 + (\hbar^2/2)(k_x^2/m_x + k_y^2/m_y - k_z^2/m_z)$ where m_x , m_y , and m_z are positive constants. Show that when $\varepsilon \approx \varepsilon_0$, the derivative of the density of levels has the form

$$\begin{aligned} g_n'(\varepsilon) &\approx \text{constant}, & \varepsilon > \varepsilon_0; \\ &\approx (\varepsilon_0 - \varepsilon)^{-1/2}, & \varepsilon < \varepsilon_0. \end{aligned} \quad (8.82)$$

9

Electrons in a Weak Periodic Potential

Perturbation Theory and Weak Periodic Potentials

Energy Levels Near a Single Bragg Plane

Illustration of Extended-, Reduced-, and
Repeated-Zone Schemes in One Dimension

Fermi Surface and Brillouin Zones

Geometrical Structure Factor

Spin-Orbit Coupling

One can gain substantial insight into the structure imposed on the electronic energy levels by a periodic potential, if that potential is very weak. This approach might once have been regarded as an instructive, but academic, exercise. We now know, however, that in many cases this apparently unrealistic assumption gives results surprisingly close to the mark. Modern theoretical and experimental studies of the metals found in groups I, II, III, and IV of the periodic table (i.e., metals whose atomic structure consists of s and p electrons outside of a closed-shell noble gas configuration) indicate that the conduction electrons can be described as moving in what amounts to an almost constant potential. These elements are often referred to as "nearly free electron" metals, because the starting point for their description is the Sommerfeld free electron gas, modified by the presence of a *weak* periodic potential. In this chapter we shall examine some of the broad general features of band structure from the almost free electron point of view. Applications to particular metals will be examined in Chapter 15.

It is by no means obvious why the conduction bands of these metals should be so free-electron-like. There are two fundamental reasons why the strong interactions of the conduction electrons with each other and with the positive ions can have the net effect of a very weak potential.

1. The electron-ion interaction is strongest at small separations, but the conduction electrons are forbidden (by the Pauli principle) from entering the immediate neighborhood of the ions because this region is already occupied by the core electrons.
2. In the region in which the conduction electrons are allowed, their mobility further diminishes the net potential any single electron experiences, for they can *screen* the fields of positively charged ions, diminishing the total effective potential.

These remarks offer only the barest indication of why the following discussion has extensive practical application. We shall return later to the problem of justifying the nearly free electron approach, taking up point 1 in Chapter 11 and point 2 in Chapter 17.

GENERAL APPROACH TO THE SCHRÖDINGER EQUATION WHEN THE POTENTIAL IS WEAK

When the periodic potential is zero, the solutions to Schrödinger's equation are plane waves. A reasonable starting place for the treatment of weak periodic potentials is therefore the expansion of the exact solution in plane waves described in Chapter 8. The wave function of a Bloch level with crystal momentum \mathbf{k} can be written in the form given in Eq. (8.42):

$$\psi_{\mathbf{k}}(\mathbf{r}) = \sum_{\mathbf{K}} c_{\mathbf{k}-\mathbf{K}} e^{i(\mathbf{k}-\mathbf{K}) \cdot \mathbf{r}}, \quad (9.1)$$

where the coefficients $c_{\mathbf{k}-\mathbf{K}}$ and the energy of the level ε are determined by the set of Eqs. (8.41):

$$\left[\frac{\hbar^2}{2m} (\mathbf{k} - \mathbf{K})^2 - \varepsilon \right] c_{\mathbf{k}-\mathbf{K}} + \sum_{\mathbf{K}'} U_{\mathbf{K}'-\mathbf{K}} c_{\mathbf{k}-\mathbf{K}'} = 0. \quad (9.2)$$

The sum in (9.1) is over all reciprocal lattice vectors \mathbf{K} , and for fixed \mathbf{k} there is an equation of the form (9.2) for each reciprocal lattice vector \mathbf{K} . The (infinitely many) different solutions to (9.2) for a given \mathbf{k} are labeled with the band index n . The wave vector \mathbf{k} can (but need not) be considered to lie in the first Brillouin zone of k -space.

In the free electron case, all the Fourier components $U_{\mathbf{k}}$ are precisely zero. Equation (9.2) then becomes

$$(\varepsilon_{\mathbf{k}-\mathbf{K}}^0 - \varepsilon)c_{\mathbf{k}-\mathbf{K}} = 0, \quad (9.3)$$

where we have introduced the notation:

$$\varepsilon_q^0 = \frac{\hbar^2}{2m}q^2. \quad (9.4)$$

Equation (9.3) requires for each \mathbf{K} that either $c_{\mathbf{k}-\mathbf{K}} = 0$ or $\varepsilon = \varepsilon_{\mathbf{k}-\mathbf{K}}^0$. The latter possibility can occur for only a single \mathbf{K} , unless it happens that some of the $\varepsilon_{\mathbf{k}-\mathbf{K}}^0$ are equal for several different choices of \mathbf{K} . If such degeneracy does *not* occur, then we have the expected class of free electron solutions:

$$\varepsilon = \varepsilon_{\mathbf{k}-\mathbf{K}}^0, \quad \psi_{\mathbf{k}} \propto e^{i(\mathbf{k}-\mathbf{K}) \cdot \mathbf{r}}. \quad (9.5)$$

If, however, there is a group of reciprocal lattice vectors $\mathbf{K}_1, \dots, \mathbf{K}_m$ satisfying

$$\varepsilon_{\mathbf{k}-\mathbf{K}_1}^0 = \dots = \varepsilon_{\mathbf{k}-\mathbf{K}_m}^0, \quad (9.6)$$

then when ε is equal to the common value of these free electron energies there are m independent degenerate plane wave solutions. Since any linear combination of degenerate solutions is also a solution, one has complete freedom in choosing the coefficients $c_{\mathbf{k}-\mathbf{K}}$ for $\mathbf{K} = \mathbf{K}_1, \dots, \mathbf{K}_m$.

These simple observations acquire more substance when the $U_{\mathbf{k}}$ are not zero, but very small. The analysis still divides naturally into two cases, corresponding to the nondegenerate and degenerate cases for free electrons. Now, however, the basis for the distinction is not the exact equality¹ of two or more distinct free electron levels, but only whether they are equal aside from terms of order U .

Case I Fix \mathbf{k} and consider a particular reciprocal lattice vector \mathbf{K}_1 such that the free electron energy $\varepsilon_{\mathbf{k}-\mathbf{K}_1}^0$ is far from the values of $\varepsilon_{\mathbf{k}-\mathbf{K}}^0$ (for all other \mathbf{K}) compared with U (see Figure 9.1)²:

$$|\varepsilon_{\mathbf{k}-\mathbf{K}_1}^0 - \varepsilon_{\mathbf{k}-\mathbf{K}}^0| \gg U, \quad \text{for fixed } \mathbf{k} \text{ and all } \mathbf{K} \neq \mathbf{K}_1. \quad (9.7)$$

We wish to investigate the effect of the potential on that free electron level given by:

$$\varepsilon = \varepsilon_{\mathbf{k}-\mathbf{K}_1}^0, \quad c_{\mathbf{k}-\mathbf{K}} = 0, \quad \mathbf{K} \neq \mathbf{K}_1. \quad (9.8)$$

¹ The reader familiar with stationary perturbation theory may think that if there is no exact degeneracy, we can always make all level differences large compared with U by considering sufficiently small U . That is indeed true for any given \mathbf{k} . However, once we are given a definite U , no matter how small, we want a procedure valid for all \mathbf{k} in the first Brillouin zone. We shall see that no matter how small U is we can always find some values of \mathbf{k} for which the unperturbed levels are closer together than U . Therefore what we are doing is more subtle than conventional degenerate perturbation theory.

² In inequalities of this form we shall use U to refer to a typical Fourier component of the potential.

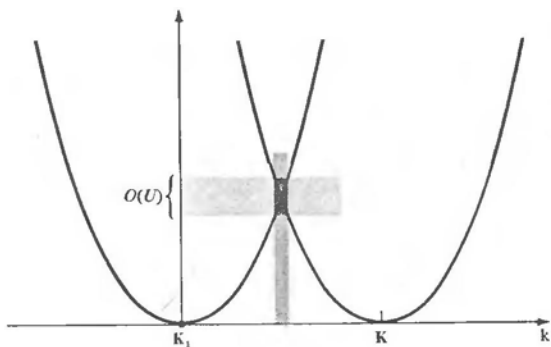


Figure 9.1

For the range of k within limits indicated by the dark band the free electron levels ε_{k-k_1} and ε_{k-k} differ by an energy $O(U)$.

Setting $K = K_1$ in Eq. (9.2) (and using the short notation (9.4)) we have (dropping the prime from the summation index):

$$(\varepsilon - \varepsilon_{k-K_1}^0)c_{k-K_1} = \sum_K U_{K-K_1}c_{k-K}. \quad (9.9)$$

Because we have picked the additive constant in the potential energy so that $U_K = 0$ when $K = 0$ (see page 137), only terms with $K \neq K_1$ appear on the right-hand side of (9.9). Since we are examining that solution for which c_{k-K} vanishes when $K \neq K_1$ in the limit of vanishing U , we expect the right-hand side of (9.9) to be of second order in U . This can be explicitly confirmed by writing Eq. (9.2) for $K \neq K_1$ as

$$c_{k-K} = \frac{U_{K_1-K}c_{k-K_1}}{\varepsilon - \varepsilon_{k-K}^0} + \sum_{K' \neq K_1} \frac{U_{K'-K}c_{k-K'}}{\varepsilon - \varepsilon_{k-K}^0}. \quad (9.10)$$

We have separated out of the sum in (9.10) the term containing c_{k-K_1} , since it will be an order of magnitude larger than the remaining terms, which involve $c_{k-K'}$ for $K' \neq K_1$. This conclusion depends on the assumption (9.7) that the level $\varepsilon_{k-K_1}^0$ is not nearly degenerate to some other ε_{k-K}^0 . Such a near degeneracy could cause some of the denominators in (9.10) to be of order U , canceling the explicit U in the numerator and resulting in additional terms in the sum in (9.10) comparable to the $K = K_1$ term.

Therefore, provided there is no near degeneracy,

$$c_{k-K} = \frac{U_{K_1-K}c_{k-K_1}}{\varepsilon - \varepsilon_{k-K}^0} + O(U^2). \quad (9.11)$$

Placing this in (9.9), we find:

$$(\varepsilon - \varepsilon_{k-K_1}^0)c_{k-K_1} = \sum_K \frac{U_{K-K_1}U_{K_1-K}}{\varepsilon - \varepsilon_{k-K}^0} c_{k-K_1} + O(U^3). \quad (9.12)$$

Thus the perturbed energy level ε differs from the free electron value $\varepsilon_{k-K_1}^0$ by terms of order U^2 . To solve Eq. (9.12) for ε to this order, it therefore suffices to replace

the ε appearing in the denominator on the right-hand side by $\varepsilon_{k-k_1}^0$, leading to the following expression³ for ε , correct to second order in U :

$$\varepsilon = \varepsilon_{k-k_1}^0 + \sum_{\mathbf{K}} \frac{|U_{\mathbf{k}-\mathbf{K}_1}|^2}{\varepsilon_{k-k_1}^0 - \varepsilon_{k-\mathbf{K}}^0} + O(U^3). \quad (9.13)$$

Equation (9.13) asserts that weakly perturbed nondegenerate bands repel each other, for every level $\varepsilon_{k-\mathbf{K}}^0$ that lies below $\varepsilon_{k-k_1}^0$ contributes a term in (9.13) that raises the value of ε , while every level that lies above $\varepsilon_{k-k_1}^0$ contributes a term that lowers the energy. However, the most important feature to emerge from this analysis of the case of no near degeneracy, is simply the gross observation that the shift in energy from the free electron value is second order in U . In the nearly degenerate case (as we shall now see) the shift in energy can be linear in U . Therefore, to leading order in the weak periodic potential, it is only the nearly degenerate free electron levels that are significantly shifted, and we must devote most of our attention to this important case.

Case 2 Suppose the value of \mathbf{k} is such that there are reciprocal lattice vectors $\mathbf{K}_1, \dots, \mathbf{K}_m$ with $\varepsilon_{k-\mathbf{K}_1}^0, \dots, \varepsilon_{k-\mathbf{K}_m}^0$ all within order U of each other,⁴ but far apart from the other $\varepsilon_{k-\mathbf{K}}^0$ on the scale of U :

$$|\varepsilon_{k-\mathbf{K}}^0 - \varepsilon_{k-\mathbf{K}_i}^0| \gg U, \quad i = 1, \dots, m, \quad \mathbf{K} \neq \mathbf{K}_1, \dots, \mathbf{K}_m. \quad (9.14)$$

In this case we must treat separately those equations given by (9.2) when \mathbf{K} is set equal to any of the m values $\mathbf{K}_1, \dots, \mathbf{K}_m$. This gives m equations corresponding to the single equation (9.9) in the nondegenerate case. In these m equations we separate from the sum those terms containing the coefficients $c_{k-\mathbf{K}_j}$, $j = 1, \dots, m$, which need not be small in the limit of vanishing interaction, from the remaining $c_{k-\mathbf{K}}$, which will be at most of order U . Thus we have

$$(\varepsilon - \varepsilon_{k-\mathbf{K}_i}^0)c_{k-\mathbf{K}_i} = \sum_{j=1}^m U_{\mathbf{K}_j-\mathbf{K}_i} c_{k-\mathbf{K}_j} + \sum_{\mathbf{K} \neq \mathbf{K}_1, \dots, \mathbf{K}_m} U_{\mathbf{K}-\mathbf{K}_i} c_{k-\mathbf{K}}, \quad i = 1, \dots, m. \quad (9.15)$$

Making the same separation in the sum, we can write Eq. (9.2) for the remaining levels as

$$c_{k-\mathbf{K}} = \frac{1}{\varepsilon - \varepsilon_{k-\mathbf{K}}^0} \left(\sum_{j=1}^m U_{\mathbf{K}_j-\mathbf{K}} c_{k-\mathbf{K}_j} + \sum_{\mathbf{K}' \neq \mathbf{K}_1, \dots, \mathbf{K}_m} U_{\mathbf{K}'-\mathbf{K}} c_{k-\mathbf{K}'} \right), \quad \mathbf{K} \neq \mathbf{K}_1, \dots, \mathbf{K}_m, \quad (9.16)$$

(which corresponds to equation (9.10) in the case of no near degeneracy).

Since $c_{k-\mathbf{K}}$ will be at most of order U when $\mathbf{K} \neq \mathbf{K}_1, \dots, \mathbf{K}_m$, Eq. (9.16) gives

$$c_{k-\mathbf{K}} = \frac{1}{\varepsilon - \varepsilon_{k-\mathbf{K}}^0} \sum_{j=1}^m U_{\mathbf{K}_j-\mathbf{K}} c_{k-\mathbf{K}_j} + O(U^2). \quad (9.17)$$

³ We use Eq. (8.34), $U_{-\mathbf{K}} = U_{\mathbf{K}}^*$.

⁴ In one dimension m cannot exceed 2, but in three dimensions it can be quite large.

Placing this in (9.15), we find that

$$(\varepsilon - \varepsilon_{k-k_i}^0)c_{k-k_i} = \sum_{j=1}^m U_{k_j-k_i}c_{k-k_j} + \sum_{j=1}^m \left(\sum_{\mathbf{K} \neq \mathbf{K}_1, \dots, \mathbf{K}_m} \frac{U_{\mathbf{K}-k_i} U_{\mathbf{K}-\mathbf{K}}}{\varepsilon - \varepsilon_{\mathbf{K}-\mathbf{K}}^0} \right) c_{k-k_j} + O(U^3). \quad (9.18)$$

Compare this with the result (9.12) in the case of no near degeneracy. There we found an explicit expression for the shift in energy to order U^2 (to which the set of equations (9.18) reduces when $m = 1$). Now, however, we find that to an accuracy of order U^2 the determination of the shifts in the m nearly degenerate levels reduces to the solution of m coupled equations⁵ for the c_{k-k_j} . Furthermore, the coefficients in the second term on the right-hand side of these equations are of higher order in U than those in the first.⁶ Consequently, to find the *leading* corrections in U we can replace (9.18) by the far simpler equations:

$$(\varepsilon - \varepsilon_{k-k_i}^0)c_{k-k_i} = \sum_{j=1}^m U_{k_j-k_i}c_{k-k_j}, \quad i = 1, \dots, m, \quad (9.19)$$

which are just the general equations for a system of m quantum levels.⁷

ENERGY LEVELS NEAR A SINGLE BRAGG PLANE

The simplest and most important example of the preceding discussion is when two free electron levels are within order U of each other, but far compared with U from all other levels. When this happens, Eq. (9.19) reduces to the two equations:

$$\begin{aligned} (\varepsilon - \varepsilon_{k-k_1}^0)c_{k-k_1} &= U_{k_2-k_1}c_{k-k_2}, \\ (\varepsilon - \varepsilon_{k-k_2}^0)c_{k-k_2} &= U_{k_1-k_2}c_{k-k_1}. \end{aligned} \quad (9.20)$$

When only two levels are involved, there is little point in continuing with the notational convention that labels them symmetrically. We therefore introduce variables particularly convenient for the two-level problem:

$$\mathbf{q} = \mathbf{k} - \mathbf{K}_1 \quad \text{and} \quad \mathbf{K} = \mathbf{K}_2 - \mathbf{K}_1, \quad (9.21)$$

and write (9.20) as

$$\begin{aligned} (\varepsilon - \varepsilon_{\mathbf{q}}^0)c_{\mathbf{q}} &= U_{\mathbf{K}}c_{\mathbf{q}-\mathbf{K}}, \\ (\varepsilon - \varepsilon_{\mathbf{q}-\mathbf{K}}^0)c_{\mathbf{q}-\mathbf{K}} &= U_{-\mathbf{K}}c_{\mathbf{q}} = U_{\mathbf{K}}^*c_{\mathbf{q}}. \end{aligned} \quad (9.22)$$

⁵ These are rather closely related to the equations of *second-order degenerate* perturbation theory, to which they reduce when all the $\varepsilon_{k-k_i}^0$ are rigorously equal, $i = 1, \dots, m$. (See L. D. Landau and E. M. Lifshitz, *Quantum Mechanics*, Addison-Wesley, Reading Mass., 1965, p. 134.)

⁶ The numerator is explicitly of order U^2 , and since only \mathbf{K} -values different from $\mathbf{K}_1, \dots, \mathbf{K}_m$ appear in the sum, the denominator is not of order U when ε is close to the $\varepsilon_{k-k_i}^0$, $i = 1, \dots, m$.

⁷ Note that the rule of thumb for going from (9.19) back to the more accurate form in (9.18) is simply that U should be replaced by U' , where

$$U'_{k_j-k_i} = U_{k_j-k_i} + \sum_{\mathbf{K} \neq \mathbf{K}_1, \dots, \mathbf{K}_m} \frac{U_{\mathbf{K}-\mathbf{K}} U_{\mathbf{K}-k_i}}{\varepsilon - \varepsilon_{\mathbf{K}-\mathbf{K}}^0}.$$

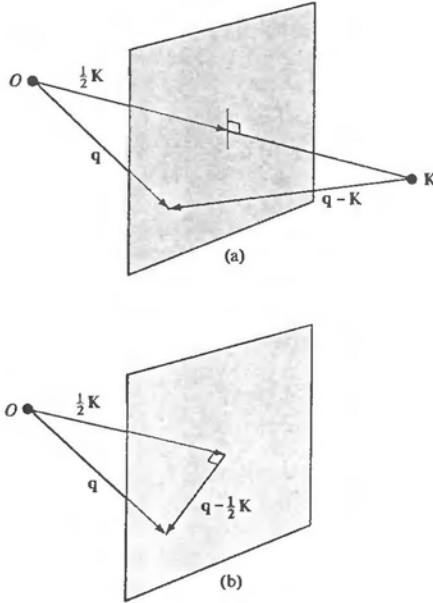
We have:

$$\varepsilon_q^0 \approx \varepsilon_{q-K}^0, \quad |\varepsilon_q^0 - \varepsilon_{q-K}^0| \gg U, \quad \text{for } K' \neq K, 0. \quad (9.23)$$

Now ε_q^0 is equal to ε_{q-K}^0 for some reciprocal lattice vector only when $|q| = |q - K|$. This means (Figure 9.2a) that q must lie on the Bragg plane (see Chapter 6) bisecting the line joining the origin of k space to the reciprocal lattice point K . The assertion that $\varepsilon_q^0 = \varepsilon_{q-K}^0$ only for $K' = K$ requires that q lie *only* on this Bragg plane, and on no other.

Figure 9.2

- (a) If $|q| = |q - K|$, then the point q must lie in the Bragg plane determined by K .
 (b) If the point q lies in the Bragg plane, then the vector $q - \frac{1}{2}K$ is parallel to the plane.



Thus conditions (9.23) have the geometric significance of requiring q to be close to a Bragg plane (but not close to a place where *two* or more Bragg planes intersect). Therefore the case of two nearly degenerate levels applies to an electron whose wave vector very nearly satisfies the condition for a single Bragg scattering.⁸ Correspondingly, the general case of many nearly degenerate levels applies to the treatment of a free electron level whose wave vector is close to one at which many simultaneous Bragg reflections can occur. Since the nearly degenerate levels are the most strongly affected by a weak periodic potential, we conclude that *a weak periodic potential has its major effects on only those free electron levels whose wave vectors are close to ones at which Bragg reflections can occur.*

We discuss systematically on pages 162 to 166 when free electron wave vectors do, or do not, lie on Bragg planes, as well as the general structure this imposes on the energy levels in a weak potential. First, however, we examine the level structure

⁸ An incident X-ray beam undergoes Bragg reflection only if its wave vector lies on a Bragg plane (see Chapter 6).

when only a single Bragg plane is nearby, as determined by (9.22). These equations have a solution when:

$$\begin{vmatrix} \varepsilon - \varepsilon_q^0 & -U_K \\ -U_K^* & \varepsilon - \varepsilon_{q-K}^0 \end{vmatrix} = 0. \quad (9.24)$$

This leads to a quadratic equation

$$(\varepsilon - \varepsilon_q^0)(\varepsilon - \varepsilon_{q-K}^0) = |U_K|^2. \quad (9.25)$$

The two roots

$$\varepsilon = \frac{1}{2}(\varepsilon_q^0 + \varepsilon_{q-K}^0) \pm \left[\left(\frac{\varepsilon_q^0 - \varepsilon_{q-K}^0}{2} \right)^2 + |U_K|^2 \right]^{1/2} \quad (9.26)$$

give the dominant effect of the periodic potential on the energies of the two free electron levels ε_q^0 and ε_{q-K}^0 when q is close to the Bragg plane determined by K . These are plotted in Figure 9.3.

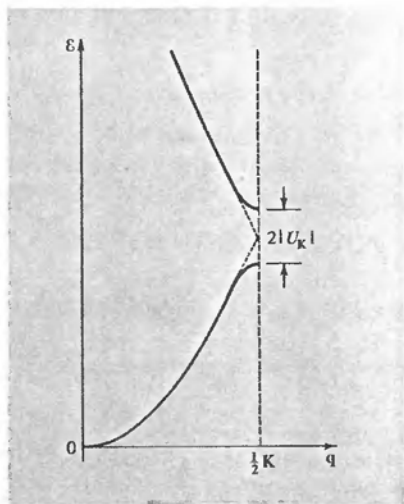


Figure 9.3

Plot of the energy bands given by Eq. (9.26) for q parallel to K . The lower band corresponds to the choice of a minus sign in (9.26) and the upper band to a plus sign. When $q = \frac{1}{2}K$, the two bands are separated by a band gap of magnitude $2|U_K|$. When q is far removed from the Bragg plane, the levels (to leading order) are indistinguishable from their free electron values (denoted by dotted lines).

The result (9.26) is particularly simple for points lying on the Bragg plane since, when q is on the Bragg plane, $\varepsilon_q^0 = \varepsilon_{q-K}^0$. Hence

$$\varepsilon = \varepsilon_q^0 \pm |U_K|, \quad q \text{ on a single Bragg plane.} \quad (9.27)$$

Thus, at all points on the Bragg plane, one level is uniformly raised by $|U_K|$ and the other is uniformly lowered by the same amount.

It is also easily verified from (9.26) that when $\varepsilon_q^0 = \varepsilon_{q-K}^0$,

$$\frac{\partial \varepsilon}{\partial q} = \frac{\hbar^2}{m} (q - \frac{1}{2}K); \quad (9.28)$$

i.e., when the point q is on the Bragg plane the gradient of ε is parallel to the plane (see Figure 9.2b). Since the gradient is perpendicular to the surfaces on which a

function is constant, the constant-energy surfaces at the Bragg plane are perpendicular to the plane.⁹

When q lies on a single Bragg plane we may also easily determine the form of the wave functions corresponding to the two solutions $\varepsilon = \varepsilon_q^0 \pm |U_K|$. From (9.22), when ε is given by (9.27), the two coefficients c_q and c_{q-K} satisfy¹⁰

$$c_q = \pm \operatorname{sgn}(U_K) c_{q-K}. \quad (9.29)$$

Since these two coefficients are the dominant ones in the plane-wave expansion (9.1), it follows that if $U_K > 0$, then

$$\begin{aligned} |\psi(\mathbf{r})|^2 &\propto (\cos \frac{1}{2}\mathbf{K} \cdot \mathbf{r})^2, & \varepsilon &= \varepsilon_q^0 + |U_K|, \\ |\psi(\mathbf{r})|^2 &\propto (\sin \frac{1}{2}\mathbf{K} \cdot \mathbf{r})^2, & \varepsilon &= \varepsilon_q^0 - |U_K|, \end{aligned}$$

while if $U_K < 0$, then

$$\begin{aligned} |\psi(\mathbf{r})|^2 &\propto (\sin \frac{1}{2}\mathbf{K} \cdot \mathbf{r})^2, & \varepsilon &= \varepsilon_q^0 + |U_K|, \\ |\psi(\mathbf{r})|^2 &\propto (\cos \frac{1}{2}\mathbf{K} \cdot \mathbf{r})^2, & \varepsilon &= \varepsilon_q^0 - |U_K|. \end{aligned} \quad (9.30)$$

Sometimes the two types of linear combination are called “*p*-like” ($|\psi|^2 \sim \sin^2 \frac{1}{2}\mathbf{K} \cdot \mathbf{r}$) and “*s*-like” ($|\psi|^2 \sim \cos^2 \frac{1}{2}\mathbf{K} \cdot \mathbf{r}$) because of their position dependence near lattice points. The *s*-like combination, like an atomic *s*-level, does not vanish at the ion; in the *p*-like combination the charge density vanishes as the square of the distance from the ion for small distances, which is also a characteristic of atomic *p*-levels.

ENERGY BANDS IN ONE DIMENSION

We can illustrate these general conclusions in one dimension, where twofold degeneracy is the most that can ever occur. In the absence of any interaction the electronic energy levels are just a parabola in k (Figure 9.4a). To leading order in the weak one-dimensional periodic potential this curve remains correct except near Bragg “planes” (which are points in one dimension). When q is near a Bragg “plane” corresponding to the reciprocal lattice vector K (i.e., the point $\frac{1}{2}K$) the corrected energy levels are determined by drawing another free electron parabola centered around K (Figure 9.4b), noting that the degeneracy at the point of intersection is split by $2|U_K|$ in such a way that both curves have zero slope at that point, and redrawing Figure 9.4b to get Figure 9.4c. The original free electron curve is therefore modified as in Figure 9.4d. When all Bragg planes and their associated Fourier components are included, we end up with a set of curves such as those shown in Figure 9.4e. This particular way of depicting the energy levels is known as the *extended-zone scheme*.

If we insist on specifying all the levels by a wave vector k in the first Brillouin zone, then we must translate the pieces of Figure 9.4e, through reciprocal lattice vectors, into the first Brillouin zone. The result is shown in Figure 9.4f. The representation is that of the *reduced-zone scheme* (see page 142).

⁹ This result is often, but not always, true even when the periodic potential is not weak, because the Bragg planes occupy positions of fairly high symmetry.

¹⁰ For simplicity we assume here that U_K is real (the crystal has inversion symmetry).

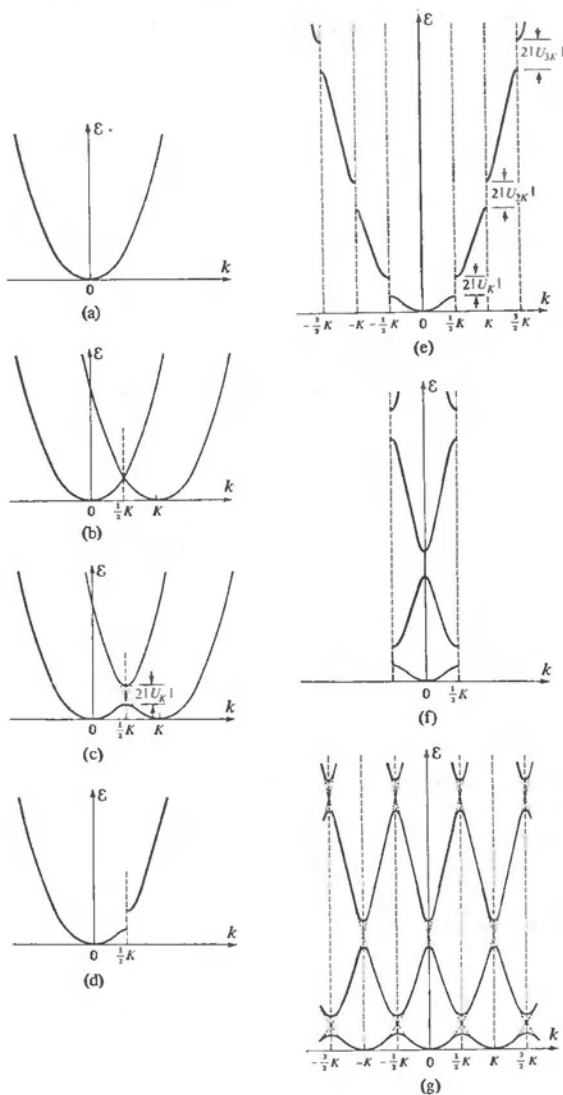


Figure 9.4

(a) The free electron ϵ vs. k parabola in one dimension. (b) Step 1 in the construction to determine the distortion in the free electron parabola in the neighborhood of a Bragg "plane," due to a weak periodic potential. If the Bragg "plane" is that determined by K , a second free electron parabola is drawn, centered on K . (c) Step 2 in the construction to determine the distortion in the free electron parabola in the neighborhood of a Bragg "plane." The degeneracy of the two parabolas at $K/2$ is split. (d) Those portions of part (c) corresponding to the original free electron parabola given in (a). (e) Effect of all additional Bragg "planes" on the free electron parabola. This particular way of displaying the electronic levels in a periodic potential is known as the *extended-zone scheme*. (f) The levels of (e), displayed in a *reduced-zone scheme*. (g) Free electron levels of (e) or (f) in a *repeated-zone scheme*.

One can also emphasize the periodicity of the labeling in k -space by periodically extending Figure 9.4f throughout all of k -space to arrive at Figure 9.4g, which emphasizes that a particular level at k can be described by any wave vector differing from k by a reciprocal lattice vector. This representation is the *repeated-zone scheme* (see page 142). The reduced-zone scheme indexes each level with a k lying in the first zone, while the extended-zone scheme uses a labeling emphasizing continuity with the free electron levels. The repeated-zone scheme is the most general representation,

but is highly redundant, since the same level is shown many times, for all equivalent wave vectors $k, k \pm K, k \pm 2K, \dots$

ENERGY-WAVE-VECTOR CURVES IN THREE DIMENSIONS

In three dimensions the structure of the energy bands is sometimes displayed by plotting ε vs. k along particular straight lines in k -space. Such curves are generally shown in a reduced-zone scheme, since for general directions in k -space they are not periodic. Even in the completely free electron approximation these curves are surprisingly complex. An example is shown in Figure 9.5, which was constructed by plotting, as k varied along the particular lines shown, the values of $\varepsilon_{\mathbf{k}-\mathbf{K}}^0 = \hbar^2(\mathbf{k} - \mathbf{K})^2/2m$ for all reciprocal lattice vectors \mathbf{K} close enough to the origin to lead to energies lower than the top of the vertical scale.

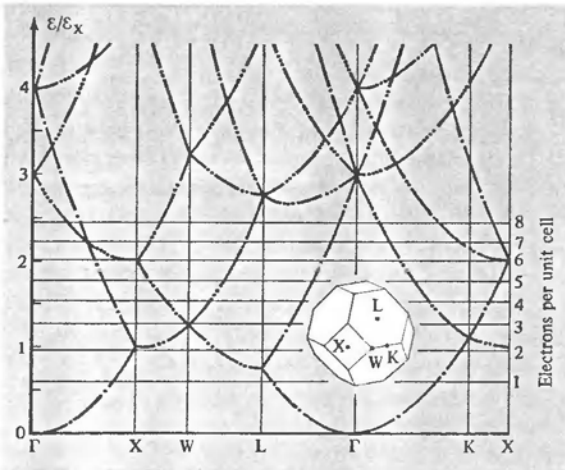


Figure 9.5

Free electron energy levels for an fcc Bravais lattice. The energies are plotted along lines in the first Brillouin zone joining the points $\Gamma(\mathbf{k} = 0)$, K , L , W , and X . ε_x is the energy at point X ($[\hbar^2/2m][2\pi/a]^2$). The horizontal lines give Fermi energies for the indicated numbers of electrons per primitive cell. The number of dots on a curve specifies the number of degenerate free electron levels represented by the curve. (From F. Herman, in *An Atomistic Approach to the Nature and Properties of Materials*, J. A. Pask, ed., Wiley, New York, 1967.)

Note that most of the curves are highly degenerate. This is because the directions along which the energy has been plotted are all lines of fairly high symmetry, so points along them are likely to be as far from several other reciprocal lattice vectors as they are from any given one. The addition of a weak periodic potential will in general remove some, but not necessarily all, of this degeneracy. The mathematical theory of groups is often used to determine how such degeneracies will be split.

THE ENERGY GAP

Quite generally, a weak periodic potential introduces an “energy gap” at Bragg planes. By this we mean the following:

When $U_{\mathbf{k}} = 0$, as \mathbf{k} crosses a Bragg plane the energy changes continuously from the lower root of (9.26) to the upper, as illustrated in Figure 9.4b. When $U_{\mathbf{k}} \neq 0$, this is no longer so. The energy only changes continuously with \mathbf{k} , as the Bragg plane is crossed, if one stays with the lower (or upper) root, as illustrated in Figure 9.4c. To change branches as \mathbf{k} varies continuously it is now necessary for the energy to change *discontinuously* by at least $2|U_{\mathbf{k}}|$.

We shall see in Chapter 12 that this mathematical separation of the two bands is reflected in a physical separation: When the action of an external field changes an electron's wave vector, the presence of the energy gap requires that upon crossing the Bragg plane, the electron must emerge in a level whose energy remains in the original branch of $\mathcal{E}(\mathbf{k})$. It is this property that makes the energy gap of fundamental importance in electronic transport properties.

BRILLOUIN ZONES

Using the theory of electrons in a weak periodic potential to determine the complete band structure of a three-dimensional crystal leads to geometrical constructions of great complexity. It is often most important to determine the Fermi surface (page 141) and the behavior of the $\mathcal{E}_n(\mathbf{k})$ in its immediate vicinity.

In doing this for weak potentials, the procedure is first to draw the free electron Fermi sphere centered at $\mathbf{k} = 0$. Next, one notes that the sphere will be deformed in a manner of which Figure 9.6 is characteristic¹¹ when it crosses a Bragg plane and in a correspondingly more complex way when it passes near several Bragg planes. When the effects of all Bragg planes are inserted, this leads to a representation of the Fermi surface as a fractured sphere in the extended-zone scheme. To construct the portions of the Fermi surface lying in the various bands in the repeated-zone scheme one can make a similar construction, starting with free electron spheres centered about all reciprocal lattice points. To construct the Fermi surface in the reduced-zone scheme, one can translate all the pieces of the single fractured sphere back into the first zone through reciprocal lattice vectors. This procedure is made systematic through the geometrical notion of the higher Brillouin zones.

Recall that the first Brillouin zone is the Wigner-Seitz primitive cell of the reciprocal lattice (pages 73 and 89), i.e. the set of points lying closer to $\mathbf{K} = 0$ than to any other

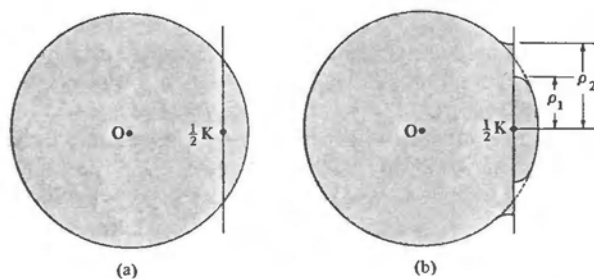


Figure 9.6

(a) Free electron sphere cutting Bragg plane located at $\frac{1}{2}K$ from the origin ($U_{\mathbf{k}} = 0$).
 (b) Deformation of the free electron sphere near the Bragg plane when $U_{\mathbf{k}} \neq 0$. The constant-energy surface intersects the plane in two circles, whose radii are calculated in Problem 1.

¹¹ This follows from the demonstration on page 159 that a constant-energy surface is perpendicular to a Bragg plane when they intersect, in the nearly free electron approximation.

reciprocal lattice point. Since Bragg planes bisect the lines joining the origin to points of the reciprocal lattice, one can equally well define the first zone as the set of points that can be reached from the origin without crossing any Bragg planes.¹²

Higher Brillouin zones are simply other regions bounded by the Bragg planes, defined as follows:

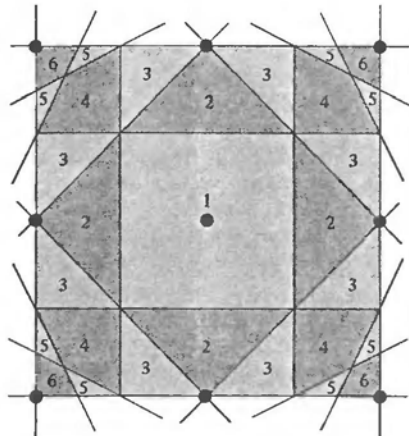
The *first Brillouin zone* is the set of points in k -space that can be reached from the origin without crossing *any* Bragg plane. The *second Brillouin zone* is the set of points that can be reached from the first zone by crossing only one Bragg plane. The $(n + 1)$ th Brillouin zone is the set of points not in the $(n - 1)$ th zone that can be reached from the n th zone by crossing only one Bragg plane.

Alternatively, the n th Brillouin zone can be defined as the set of points that can be reached from the origin by crossing $n - 1$ Bragg planes, but no fewer.

These definitions are illustrated in two dimensions in Figure 9.7. The surface of the first three zones for the fcc and bcc lattices are shown in Figure 9.8. Both definitions emphasize the physically important fact that the zones are bounded by Bragg planes. Thus they are regions at whose surfaces the effects of a weak periodic potential are important (i.e., first order), but in whose interior the free electron energy levels are only perturbed in second order.

Figure 9.7

Illustration of the definition of the Brillouin zones for a two-dimensional square Bravais lattice. The reciprocal lattice is also a square lattice of side b . The figure shows all Bragg planes (lines, in two dimensions) that lie within the square of side $2b$ centered on the origin. These Bragg planes divide that square into regions belonging to zones 1 to 6. (Only zones 1, 2, and 3 are entirely contained within the square, however.)



It is very important to note that each Brillouin zone is a primitive cell of the reciprocal lattice. This is because the n th Brillouin zone is simply the set of points that have the origin as the n th nearest reciprocal lattice point (a reciprocal lattice point \mathbf{K} is nearer to a point \mathbf{k} than \mathbf{k} is to the origin if and only if \mathbf{k} is separated from the origin by the Bragg plane determined by \mathbf{K}). Given this, the proof that the n th Brillouin zone is a primitive cell is identical to the proof on page 73 that the Wigner-Seitz cell (i.e., the first Brillouin zone) is primitive, provided that the phrase “ n th nearest neighbor” is substituted for “nearest neighbor” throughout the argument.

¹² We exclude from consideration points lying on Bragg planes, which turn out to be points common to the surface of two or more zones. We define the zones in terms of their interior points.

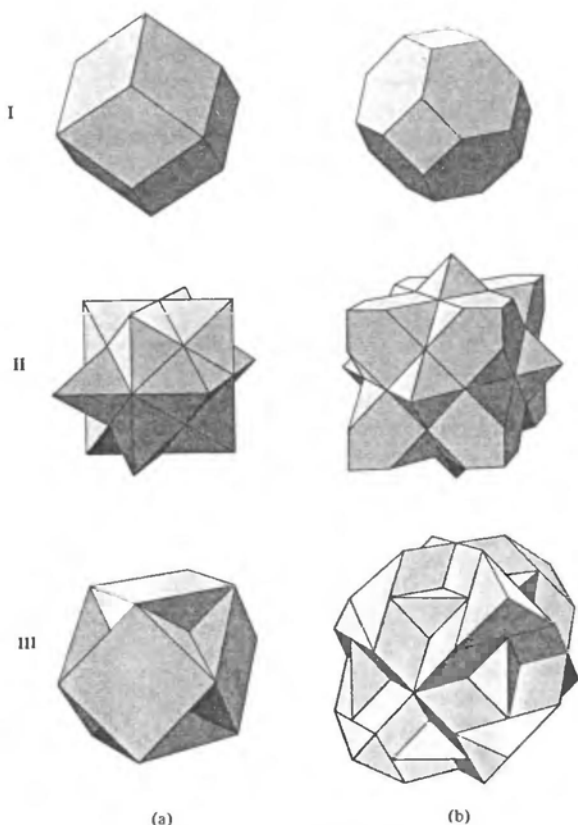


Figure 9.8

Surfaces of the first, second, and third Brillouin zones for (a) body-centered cubic and (b) face-centered cubic crystals. (Only the exterior surfaces are shown. It follows from the definition on page 163 that the interior surface of the n th zone is identical to the exterior surface of the $(n - 1)$ th zone.) Evidently the surfaces bounding the zones become increasingly complex as the zone number increases. In practice it is often simplest to construct free electron Fermi surfaces by procedures (such as those described in Problem 4) that avoid making use of the explicit form of the Brillouin zones. (After R. Lück, doctoral dissertation, Technische Hochschule, Stuttgart, 1965.)

Because each zone is a primitive cell, there is a simple algorithm for constructing the branches of the Fermi surface in the repeated-zone scheme¹³:

1. Draw the free electron Fermi sphere.
2. Deform it slightly (as illustrated in Figure 9.6) in the immediate vicinity of every Bragg plane. (In the limit of exceedingly weak potentials this step is sometimes ignored to a first approximation.)
3. Take that portion of the surface of the free electron sphere lying within the n th Brillouin zone, and translate it through all reciprocal lattice vectors. The resulting surface is the branch of the Fermi surface (conventionally assigned to the n th band) in the repeated-zone scheme.¹⁴

¹³ The representation of the Fermi surface in the repeated-zone scheme is the most general. After surveying each branch in its full periodic splendor, one can pick that primitive cell which most lucidly represents the topological structure of the whole (which is often, but by no means always, the first Brillouin zone).

¹⁴ An alternative procedure is to translate the pieces of the Fermi surface in the n th zone through those reciprocal lattice vectors that take the pieces of the n th zone in which they are contained, into the first zone. (Such translations exist because the n th zone is a primitive cell.) This is illustrated in Figure 9.9. The Fermi surface in the repeated-zone scheme is then constructed by translating the resulting first zone structures through all reciprocal lattice vectors.

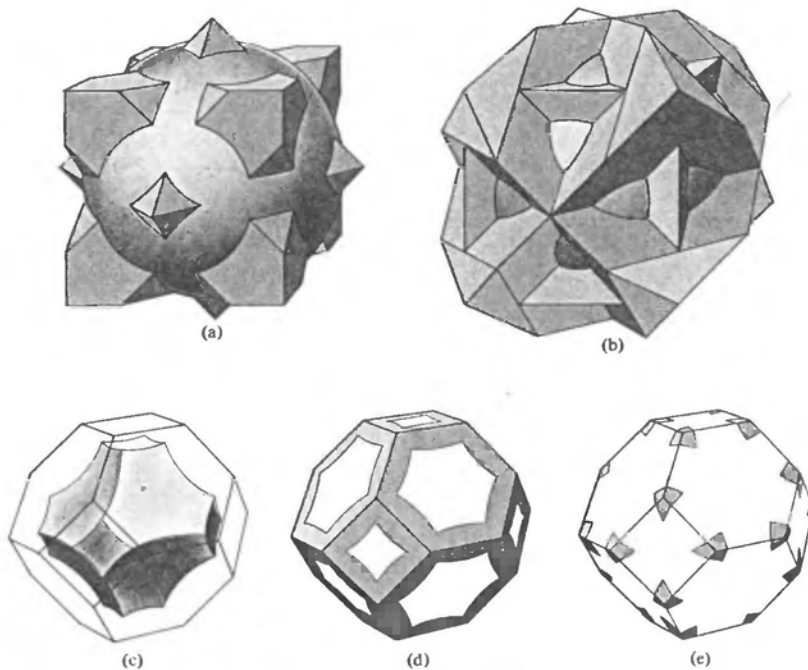


Figure 9.9

The free electron Fermi sphere for a face-centered cubic metal of valence 4. The first zone lies entirely within the interior of the sphere, and the sphere does not extend beyond the fourth zone. Thus the only zone surfaces intersected by the surface of the sphere are the (exterior) surfaces of the second and third zones (cf. Figure 9.8b). The second-zone Fermi surface consists of those parts of the surface of the sphere lying entirely within the polyhedron bounding the second zone (i.e., all of the sphere except the parts extending beyond the polyhedron in (a)). When translated through reciprocal lattice vectors into the first zone, the pieces of the second-zone surface give the simply connected figure shown in (c). (It is known as a “hole surface”; the levels it encloses have higher energies than those outside). The third-zone Fermi surface consists of those parts of the surface of the sphere lying outside of the second zone (i.e., the parts extending beyond the polyhedron in (a)) that do not lie outside the third zone (i.e., that are contained within the polyhedron shown in (b)). When translated through reciprocal lattice vectors into the first zone, these pieces of sphere give the multiply connected structure shown in (d). The fourth-zone Fermi surface consists of the remaining parts of the surface of the sphere that lie outside the third zone (as shown in (b)). When translated through reciprocal lattice vectors into the first zone they form the “pockets of electrons” shown in (e). For clarity (d) and (e) show only the intersection of the third and fourth zone Fermi surfaces with the surface of the first zone. (From R. Lück, *op. cit.*)

Generally speaking, the effect of the weak periodic potential on the surfaces constructed from the free electron Fermi sphere without step 2, is simply to round off the sharp edges and corners. If, however, a branch of the Fermi surface consists of very small pieces of surface (surrounding either occupied or unoccupied levels, known as “pockets of electrons” or “pockets of holes”), then a weak periodic potential may cause these to disappear. In addition, if the free electron Fermi surface has parts with a very narrow cross section, a weak periodic potential may cause it to become disconnected at such points.

Some further constructions appropriate to the discussion of almost free electrons in fcc crystals are illustrated in Figure 9.10. These free-electron-like Fermi surfaces are of great importance in understanding the real Fermi surfaces of many metals. This will be illustrated in Chapter 15.

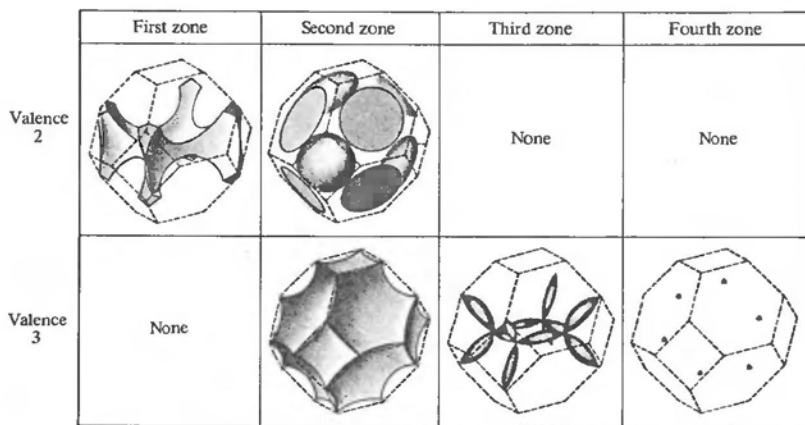


Figure 9.10

The free electron Fermi surfaces for face-centered cubic metals of valence 2 and 3. (For valence 1 the surface lies entirely within the interior of the first zone and therefore remains a sphere to lowest order; the surface for valence 4 is shown in Figure 9.9.) All branches of the Fermi surface are shown. The primitive cells in which they are displayed have the shape and orientation of the first Brillouin zone. However, the cell is actually the first zone (i.e., is centered on $\mathbf{K} = 0$) only in the figures illustrating the second zone surfaces. In the first and third zone figures $\mathbf{K} = 0$ lies at the center of one of the horizontal faces, while for the fourth zone figure it lies at the center of the hexagonal face on the upper right (or the parallel face opposite it (hidden)). The six tiny pockets of electrons constituting the fourth zone surface for valence 3 lie at the corners of the regular hexagon given by displacing that hexagonal face in the $[111]$ direction by half the distance to the face opposite it. (After W. Harrison, *Phys. Rev.* **118**, 1190 (1960).) Corresponding constructions for body-centered cubic metals can be found in the Harrison paper.

THE GEOMETRICAL STRUCTURE FACTOR IN MONATOMIC LATTICES WITH BASES

Nothing said up to now has exploited any properties of the potential $U(\mathbf{r})$ other than its periodicity, and, for convenience, inversion symmetry. If we pay somewhat

closer attention to the form of U , recognizing that it will be made up of a sum of atomic potentials centered at the positions of the ions, then we can draw some further conclusions that are important in studying the electronic structure of monatomic lattices with a basis, such as the diamond and hexagonal close-packed (hcp) structures.

Suppose that the basis consists of identical ions at positions \mathbf{d}_j . Then the periodic potential $U(\mathbf{r})$ will have the form

$$U(\mathbf{r}) = \sum_{\mathbf{R}} \sum_j \phi(\mathbf{r} - \mathbf{R} - \mathbf{d}_j). \quad (9.31)$$

If we place this into Eq. (8.32) for $U_{\mathbf{K}}$, we find that

$$\begin{aligned} U_{\mathbf{K}} &= \frac{1}{v} \int_{\text{cell}} d\mathbf{r} e^{-i\mathbf{K} \cdot \mathbf{r}} \sum_{\mathbf{R}, j} \phi(\mathbf{r} - \mathbf{R} - \mathbf{d}_j) \\ &= \frac{1}{v} \int_{\text{all space}} d\mathbf{r} e^{-i\mathbf{K} \cdot \mathbf{r}} \sum_j \phi(\mathbf{r} - \mathbf{d}_j), \end{aligned} \quad (9.32)$$

or

$$U_{\mathbf{K}} = \frac{1}{v} \phi(\mathbf{K}) S_{\mathbf{K}}^*, \quad (9.33)$$

where $\phi(\mathbf{K})$ is the Fourier transform of the atomic potential,

$$\phi(\mathbf{K}) = \int_{\text{all space}} d\mathbf{r} e^{-i\mathbf{K} \cdot \mathbf{r}} \phi(\mathbf{r}), \quad (9.34)$$

and $S_{\mathbf{K}}$ is the geometrical structure factor introduced in our discussion of X-ray diffraction (Chapter 6):

$$S_{\mathbf{K}} = \sum_j e^{i\mathbf{K} \cdot \mathbf{d}_j}. \quad (9.35)$$

Thus when the basis leads to a vanishing structure factor for some Bragg planes, i.e., when the X-ray diffraction peaks from these planes are missing, then the Fourier component of the periodic potential associated with such planes vanishes; i.e., the lowest-order splitting in the free electron levels disappears.

This result is of particular importance in the theory of metals with the hexagonal close-packed structure, of which there are over 25 (Table 4.4). The first Brillouin zone for the simple hexagonal lattice is a prism on a regular hexagon base. However, the structure factor associated with the hexagonal top and bottom of the prism vanishes (Problem 3, Chapter 6).

Therefore, according to nearly free electron theory, there is *no* first-order splitting of the free electron levels at these faces. It might appear that small splittings would still occur as a result of second-order (and higher-order) effects. However, if the one-electron Hamiltonian is independent of the spin, then in the hcp structure any Bloch level with wave vector \mathbf{k} on the hexagonal face of the first Brillouin zone can be proved to be at least twofold degenerate. Accordingly, the splitting is rigorously zero. In a situation like this it is often more convenient to consider a representation of the zone structure in which those planes with zero gap are actually ignored. The regions that one is then led to consider are known as Jones zones or large zones.

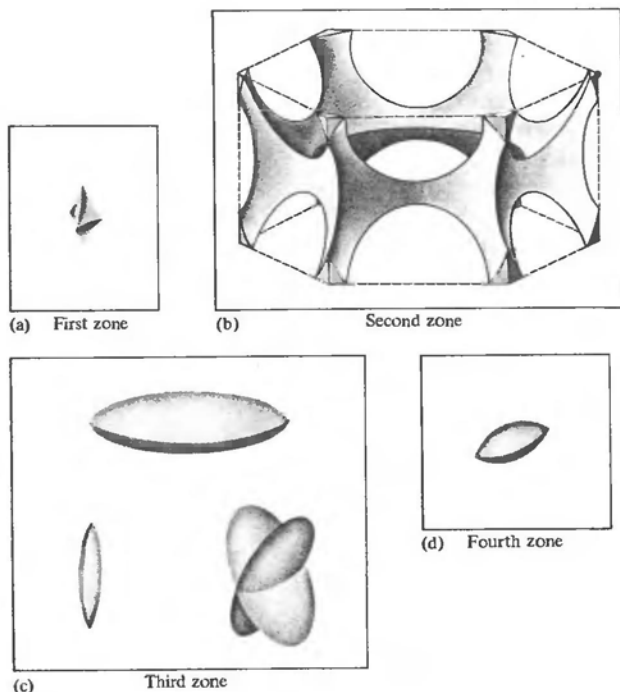


Figure 9.11

Free electron Fermi surface for a divalent hcp metal with ideal $c/a = 1.633$. Since the hcp structure is simple hexagonal with two atoms per primitive cell, there are four electrons per primitive cell to be accommodated. The resulting Fermi surface comes in many pieces, whose names reveal an interesting level of imagination and taste. (a) *The cap*. The *first zone* is almost entirely filled by the free electron sphere, but there are small unoccupied regions in the six upper and six lower corners. These can be assembled, by translations through reciprocal lattice vectors, into two of the objects shown. (b) *The monster*. Portions of the free electron sphere in the *second zone* can be translated back into the first zone to form one of the large structures shown in the second-zone picture. The monster encloses unoccupied levels. (c) Portions of the free electron sphere in the *third zone* can be reassembled into several electron-enclosing surfaces. There is one *lens*, two *cigars*, and three *butterflies*. (d) Those few occupied free electron levels in the *fourth zone* can be reassembled into three pockets of the type pictured.

These structures arise when there is significant splitting of the free electron levels on the hexagonal faces of the first zone as a result of spin-orbit coupling. When spin-orbit coupling is weak (as it is in the lighter elements), there is negligible splitting on these faces, and the appropriate structures are those shown in Figure 9.12. (From J. B. Ketterson and R. W. Stark, *Phys. Rev.* **156**, 751 (1967).)

IMPORTANCE OF SPIN-ORBIT COUPLING AT POINTS OF HIGH SYMMETRY

Until now we have regarded the electron spin as being completely inert dynamically. In fact, however, an electron moving through an electric field, such as that of the periodic potential $U(\mathbf{r})$, experiences a potential proportional to the scalar product of its spin magnetic moment with the vector product of its velocity and the electric field. This additional interaction is referred to as the *spin-orbit coupling*, and is of great importance in atomic physics (see Chapter 31). Spin-orbit coupling is important in calculating the almost free electron levels at points in k -space of high symmetry, since it often happens that levels that are rigorously degenerate when it is ignored are split by the spin-orbit coupling.

For example, the splitting of the electronic levels on the hexagonal faces of the first zone in hcp metals is entirely due to spin-orbit coupling. Since the strength of spin-orbit coupling increases with atomic number, this splitting is appreciable in the heavy hexagonal metals, but can be small enough to be ignored in the light ones. Correspondingly, there are two different schemes for constructing free electronlike Fermi surfaces in hexagonal metals. These are illustrated in Figures 9.11 and 9.12.

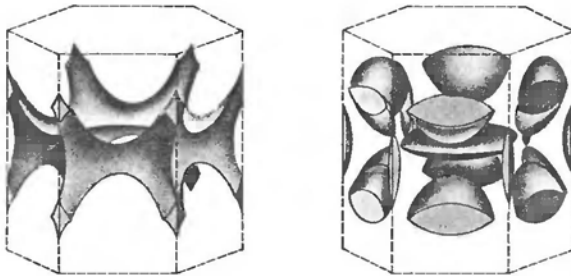


Figure 9.12

A representation of the Fermi surface of a divalent hcp metal obtained by reassembling those pieces in Figure 9.11 that were severed from each other by the horizontal hexagonal faces of the first Brillouin zone. The first and second zones together make up the structure on the left, and the many pieces in the third and fourth zones lead to the structure on the right. This representation ignores the spin orbit splitting across the hexagonal face. (After W. Harrison, *Phys. Rev.* **118**, 1190 (1960).)

PROBLEMS

1. Nearly Free Electron Fermi Surface Near a Single Bragg Plane

To investigate the nearly free electron band structure given by (9.26) near a Bragg plane, it is convenient to measure the wave vector \mathbf{q} with respect to the point $\frac{1}{2}\mathbf{K}$ on the Bragg plane. If we write $\mathbf{q} = \frac{1}{2}\mathbf{K} + \mathbf{k}$, and resolve \mathbf{k} into its components parallel (k_{\parallel}) and perpendicular (k_{\perp})

to \mathbf{K} , then (9.26) becomes

$$\varepsilon = \varepsilon_{\mathbf{k}/2}^0 + \frac{\hbar^2}{2m} k^2 \pm \left(4\varepsilon_{\mathbf{k}/2}^0 \frac{\hbar^2}{2m} k_{\parallel}^2 + |U_{\mathbf{K}}|^2 \right)^{1/2} \quad (9.36)$$

It is also convenient to measure the Fermi energy ε_F with respect to the lowest value assumed by either of the bands given by (9.36) in the Bragg plane, writing:

$$\varepsilon_F = \varepsilon_{\mathbf{k}/2}^0 - |U_{\mathbf{K}}| + \Delta, \quad (9.37)$$

so that when $\Delta < 0$, no Fermi surface intersects the Bragg plane.

(a) Show that when $0 < \Delta < 2|U_{\mathbf{K}}|$, the Fermi surface lies entirely in the lower band and intersects the Bragg plane in a circle of radius

$$\rho = \sqrt{\frac{2m\Delta}{\hbar^2}}. \quad (9.38)$$

(b) Show that if $\Delta > 2|U_{\mathbf{K}}|$, the Fermi surface lies in both bands, cutting the Bragg plane in two circles of radii ρ_1 and ρ_2 (Figure 9.6), and that the difference in the areas of the two circles is

$$\pi(\rho_2^2 - \rho_1^2) = \frac{4m\pi}{\hbar^2} |U_{\mathbf{K}}|. \quad (9.39)$$

(The area of these circles can be measured directly in some metals through the de Haas-van Alphen effect (Chapter 14), and therefore $|U_{\mathbf{K}}|$ can be determined directly from experiment for such nearly free electron metals.)

2. Density of Levels for a Two-Band Model

To some extent this problem is artificial in that the effects of neglected Bragg planes can lead to corrections comparable to the deviations we shall find here from the free electron result. On the other hand, the problem is instructive in that the qualitative features are general.

If we resolve \mathbf{q} into its components parallel (q_{\parallel}) and perpendicular (q_{\perp}) to \mathbf{K} , then (9.26) becomes

$$\varepsilon = \frac{\hbar^2}{2m} q_{\perp}^2 + h_{\pm}(q_{\parallel}), \quad (9.40)$$

where

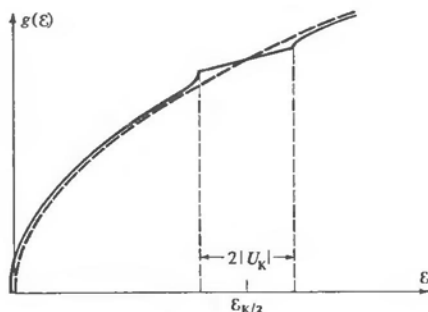
$$h_{\pm}(q_{\parallel}) = \frac{\hbar^2}{2m} \left[q_{\parallel}^2 + \frac{1}{2}(K^2 - 2q_{\parallel}K) \right] \pm \left\{ \left[\frac{\hbar^2}{2m} \frac{1}{2}(K^2 - 2q_{\parallel}K) \right]^2 + |U_{\mathbf{K}}|^2 \right\}^{1/2} \quad (9.41)$$

is only a function of q_{\parallel} . The density of levels can be evaluated from (8.57) by performing the integral in an appropriate primitive cell over wave vectors \mathbf{q} in cylindrical coordinates with the z -axis along \mathbf{K} .

(a) Show that when the integral over \mathbf{q} is performed, the result for each band is

$$g(\varepsilon) = \frac{1}{4\pi^2} \left(\frac{2m}{\hbar^2} \right) (q_{\parallel}^{\max} - q_{\parallel}^{\min}), \quad (9.42)$$

where, for each band, q_{\parallel}^{\max} and q_{\parallel}^{\min} are the solutions to $\varepsilon = h_{\pm}(q_{\parallel})$. Verify that the familiar free electron result is obtained in the limit $|U_{\mathbf{K}}| \rightarrow 0$.


Figure 9.13

Density of levels in the two-band approximation. The dashed line is the free electron result Eq. (2.63). Note that in contrast to earlier figures in this chapter, this one explicitly shows second-order corrections to the free electron result far from the Bragg plane.

(b) Show that

$$q_{\parallel}^{\min} = -\sqrt{\frac{2m\varepsilon}{\hbar^2}} + O(U_{\mathbf{k}}^2), \quad (\varepsilon > 0), \quad q_{\parallel}^{\max} = \frac{1}{2}K \quad (9.43)$$

for the lower band, if the constant energy surface (at energy ε) cuts the zone plane (that is, $\varepsilon_{\mathbf{k}/2}^0 - |U_{\mathbf{k}}| \leq \varepsilon \leq \varepsilon_{\mathbf{k}/2}^0 + |U_{\mathbf{k}}|$).

(c) Show that for the upper band (9.42) should be interpreted as giving a density of levels

$$g_+(\varepsilon) = \frac{1}{4\pi^2} \left(\frac{2m}{\hbar^2} \right) (q_{\parallel}^{\max} - \frac{1}{2}K), \quad \text{for } \varepsilon > \varepsilon_{\mathbf{k}/2} + |U_{\mathbf{k}}|. \quad (9.44)$$

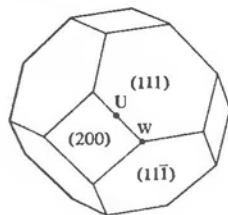
(d) Show that $dg/d\varepsilon$ is singular at $\varepsilon = \varepsilon_{\mathbf{k}/2} \pm |U_{\mathbf{k}}|$, so that the density of levels has the form shown in Figure 9.13. (These singularities are not peculiar either to the weak potential or two-band approximations. See page 145.)

3. Effect of Weak Periodic Potential at Places in k -Space Where Bragg Planes Meet

Consider the point W ($\mathbf{k}_W = (2\pi/a)(1, \frac{1}{2}, 0)$) in the Brillouin zone of the fcc structure shown (see Figure 9.14). Here three Bragg planes ((200), (111), $(11\bar{1})$) meet, and accordingly the free electron energies

$$\begin{aligned} \varepsilon_1^0 &= \frac{\hbar^2}{2m} k^2, \\ \varepsilon_2^0 &= \frac{\hbar^2}{2m} \left(\mathbf{k} - \frac{2\pi}{a} (1, 1, 1) \right)^2, \\ \varepsilon_3^0 &= \frac{\hbar^2}{2m} \left(\mathbf{k} - \frac{2\pi}{a} (1, 1, \bar{1}) \right)^2, \\ \varepsilon_4^0 &= \frac{\hbar^2}{2m} \left(\mathbf{k} - \frac{2\pi}{a} (2, 0, 0) \right)^2 \end{aligned} \quad (9.45)$$

are degenerate when $\mathbf{k} = \mathbf{k}_W$, and equal to $\varepsilon_W = \hbar^2 \mathbf{k}_W^2 / 2m$.


Figure 9.14

First Brillouin zone for a face-centered cubic crystal.

- (a) Show that in a region of
- k
- space near
- W
- , the first-order energies are given by solutions to
- ¹⁵

$$\begin{vmatrix} \varepsilon_1^0 - \varepsilon & U_1 & U_1 & U_2 \\ U_1 & \varepsilon_2^0 - \varepsilon & U_2 & U_1 \\ U_1 & U_2 & \varepsilon_3^0 - \varepsilon & U_1 \\ U_2 & U_1 & U_1 & \varepsilon_4^0 - \varepsilon \end{vmatrix} = 0$$

where $U_2 = U_{200}$, $U_1 = U_{111} = U_{11\bar{1}}$, and that at W the roots are

$$\varepsilon = \varepsilon_W - U_2 \quad (\text{twice}), \quad \varepsilon = \varepsilon_W + U_2 \pm 2U_1. \quad (9.46)$$

- (b) Using a similar method, show that the energies at the point
- U
- (
- $k_U = (2\pi/a)(1, \frac{1}{4}, \frac{1}{4})$
-) are

$$\varepsilon = \varepsilon_U - U_2, \quad \varepsilon = \varepsilon_U + \frac{1}{2}U_2 \pm \frac{1}{2}(U_2^2 + 8U_1^2)^{1/2}, \quad (9.47)$$

where $\varepsilon_U = \hbar^2 k_U^2 / 2m$.

4. Alternative Definition of Brillouin Zones

Let k be a point in reciprocal space. Suppose spheres of radius k are drawn about every reciprocal lattice point K except the origin. Show that if k is in the interior of $n - 1$ spheres, and on the surface of none, then it lies in the interior of the n th Brillouin zone. Show that if k is in the interior of $n - 1$ spheres and on the surface of m additional spheres, then it is a point common to the boundaries of the n th, $(n + 1)$ th, \dots , $(n + m)$ th Brillouin zones.

5. Brillouin Zones in a Two-Dimensional Square Lattice

Consider a two-dimensional square lattice with lattice constant a .

(a) Write down, in units of $2\pi/a$, the radius of a circle that can accommodate m free electrons per primitive cell. Construct a table listing which of the first seven zones of the square lattice (Figure 9.15a) are completely full, which are partially empty, and which are completely empty for $m = 1, 2, \dots, 12$. Verify that if $m \leq 12$, the occupied levels lie entirely within the first seven zones, and that when $m \geq 13$, levels in the eighth and higher zones become occupied.

(b) Draw pictures in suitable primitive cells of all branches of the Fermi surface for the cases $m = 1, 2, \dots, 7$. The third zone surface for $m = 4$, for example, can be displayed as in Figure 9.15b.

¹⁵ Assume that the periodic potential U has inversion symmetry so that the U_k are real.